T H E U N I V E R S I T Y O F M I C H I G A N

COLLEGE OF ENGINEERING
Department of Mechanical Engineering

Final Report

EXHAUST EMISSION CHARACTERISTICS OF OUTBOARD ENGINES

David E. Cole
Associate Professor of Mechanical Engineering

ORA Project 351920

under contract with:

OUTBOARD MARINE CORPORATION
CONTRACT NO. N-2 5-2-70
WAUKEGAN, ILLINOIS

administered through:

OFFICE OF RESEARCH ADMINISTRATION ANN ARBOR

April 1972

ensn

UMRC697

TABLE OF CONTENTS

TABLE OF CONTENTS (Concluded)

LIST OF TABLES

LIST OF FIGURES

LIST OF FIGURES (Continued)

LIST OF FIGURES (Concluded)

I. INTRODUCTION

The purpose of the past year's investigation at The University of Michigan has been to study in greater detail several important physical processes within the 2-stroke engine which may affect atmospheric pollution. Essentially this has entailed an extension of prior work directed at emission characterization and instrumentation development.

As expected the concern of all Americans for problems of the environment continue to increase at a high rate. Contrary to the early days of mass hysteria, the current movement appears to be based on more objective ground although important exceptions to this rule do exist. An important occurrence has been the more general recognition that all pollutants are not equally toxic to the environment, i.e., carbon monoxide is perhaps 200 times less toxic than the sulfur oxides on a per unit mass basis. Weighted emission scales have been developed which multiply the mass of a given pollutant emitted by a relative toxicity factor. PINDEX is a notable example of such a scale (Ref. 1). This movement is certainly good news for the engineering community and particularly for those who are engaged in the development of "clean" engines.

The 1970 Clean Air Act (Ref. 2), if fully implemented on schedule, virtually assures the removal of the automobile as an important contributor to our air pollution problem and emphasizes our statement that as the original major pollutants are brought under control those originally of lesser significance become more important. With the publication of the "Study of Exhaust Emission from Uncontrolled Vehicles and Related Equipment Using Internal Combustion

Engines" by Southwest Research Institute (EPA Contract EHS 70-108) it is highly likely that legislation will be formulated for control of most engine applications. Certainly we can expect the larger uncontrolled engines to be first on the list for control legislation. Progress reports from the Southwest Research Study suggest that most of the 2- and 4-stroke gasoline engines are high emitters. The small 4-stroke engines, while having lower HC emissions, generally exhibit higher CO levels because of richer mixture ratios. It is my opinion that publication of the final report by Southwest Research will trigger control legislation. I believe, unfortunately, that law makers will pay little heed to the fact that many of the power plants are used in regions removed from air problem areas. Realistically it is reasonable to expect that emission control of these systems will result in essentially zero improvement in the urban atmosphere. I believe it would be appropriate for OMC to publish outboard engine use data related to time of year and geographical location.

We have confined the investigation of the past year to three primary areas.

1. Misfiring study using the ion probe technique
2. Direct cylinder sampling of the charge and exhaust products
3. Two-stroke scavenging simulation.

A. ION PROBE

Our primary effort early in the past year's program was directed to the ion probe studies of misfiring or poor combustion. Instrumentation has been designed and developed which effectively allowed us to measure the degree of

flame propagation. Preliminary data showed the importance of total misfiring and partial or incomplete combustion on HC emissions at the low speed boat load conditions. At moderate and higher speeds the burning was much more complete and suggests that misfiring in this operating region is not a significant cause of HC emissions. We terminated this phase of the study in May because of the marginal value of the information compared to the potential of the other investigations.

B. DIRECT CYLINDER SAMPLING

Initially we intended to use the direct cylinder sampling system to calibrate the ion probe misfire transducer. It became apparent, however, that it could be used for a number of additional measurements and could be readily adapted for use in other engines as well. The following information can be discerned from analysis of the sample drawn through the valve:

1. HC emissions due to misfire
2. Individual cylinder F/A ratio
3. Charge homogeneity
4. Exhaust residual dilution.

Results showed that, as expected, combustion was relatively poor at light load and low speed. This can be primarily attributed to significant residual dilution of the fresh charge which was a result of inefficient scavenging. In fact, at 1000 rpm boat load the residual dilution exceeded 30%.

Variation in cylinder HC concentration (before combustion) as a function of crank angle suggested that the mixture was relatively nonhomogeneous.

C. SCAVENGING SIMULATION

In the scavenging simulation hot exhaust from a single cylinder 4-stroke cycle engine is mixed with controlled quantities of fuel/air mixture to simulate the environment to which the over scavenged mixture is exposed in the 2-cycle engine. The primary goal of this experiment is to determine the change in chemical composition of the fuel in the overscavenged mixture. Particular attention is directed at the relative reactivity of the hydrocarbons.

The hot gas mixture is ducted through a long insulated pipe in which sample probes are inserted at several intervals. Residence time of the gases is designed to be equivalent to the time required to scavenge the engine. The background HC concentration from the 4-cycle engine is low in comparison to the HC in the fuel/air mixture.

A subtractive column analyzer in conjunction with a Flame Ionization Detector (FID) is used to obtain a major family analysis of the gases (paraffins, olefins, and aromatics).

We have experienced some difficulty in achieving effective mixing of the exhaust and fuel/air mixture at the entrance of the reactor. This design is still undergoing modification to correct the problem. However, qualitative data clearly suggests that fuel composition changes little when exposed to the moderately high temperatures occurring in all but the combustion phases of the engine cycle. Therefore, it appears that the exhaust HC reactivity will be low and equivalent to the fuel/air mixture. Certainly it is much less reactive per unit of HC emission than 4-stroke exhaust which has a high olefin content.

II. TEST EQUIPMENT

A. IONIZATION PROBE

The ion probe test apparatus was discussed in Report No. 34856-2-F, 1970 (Ref. 3). A series of three mini-spark plugs were installed in cylinder No. 2 of the 100 HP Johnson test engine. Their location is shown in Figure 1 reproduced from the previous report. The distance from the spark gap to the ionization probes is shown in Figure 2.

B. CYLINDER SAMPLING SYSTEM

The principal components of the direct cylinder sampling system was the Cox, Type 5 electromagnetic sampling valve shown in Figure 3. Figure 4 shows the sampling valve installed in cylinder No. 2 of the test engine. The sample valve head was positioned .75 in. from the spark plug. With the existing head construction this proved to be the most feasible location. Even then substantial modification was necessary. For reasons which are explored in the discussion section of this report, this location is perhaps as good as any for our intended purposes. A schematic diagram of the valve is shown in Figure 5. Basically the device consists of a 15/64 in. diameter valve head with a stem which extends into and is a permeable core in an electromagnetic coil. An adjustable spring maintains the valve in contact with its seat. At a specified time in the test cycle a large capacitor is discharged through the coil and the magnetic field established attempts to eject the valve. The valve lifts approximately .012 in. from its seat and during this interval the sample is

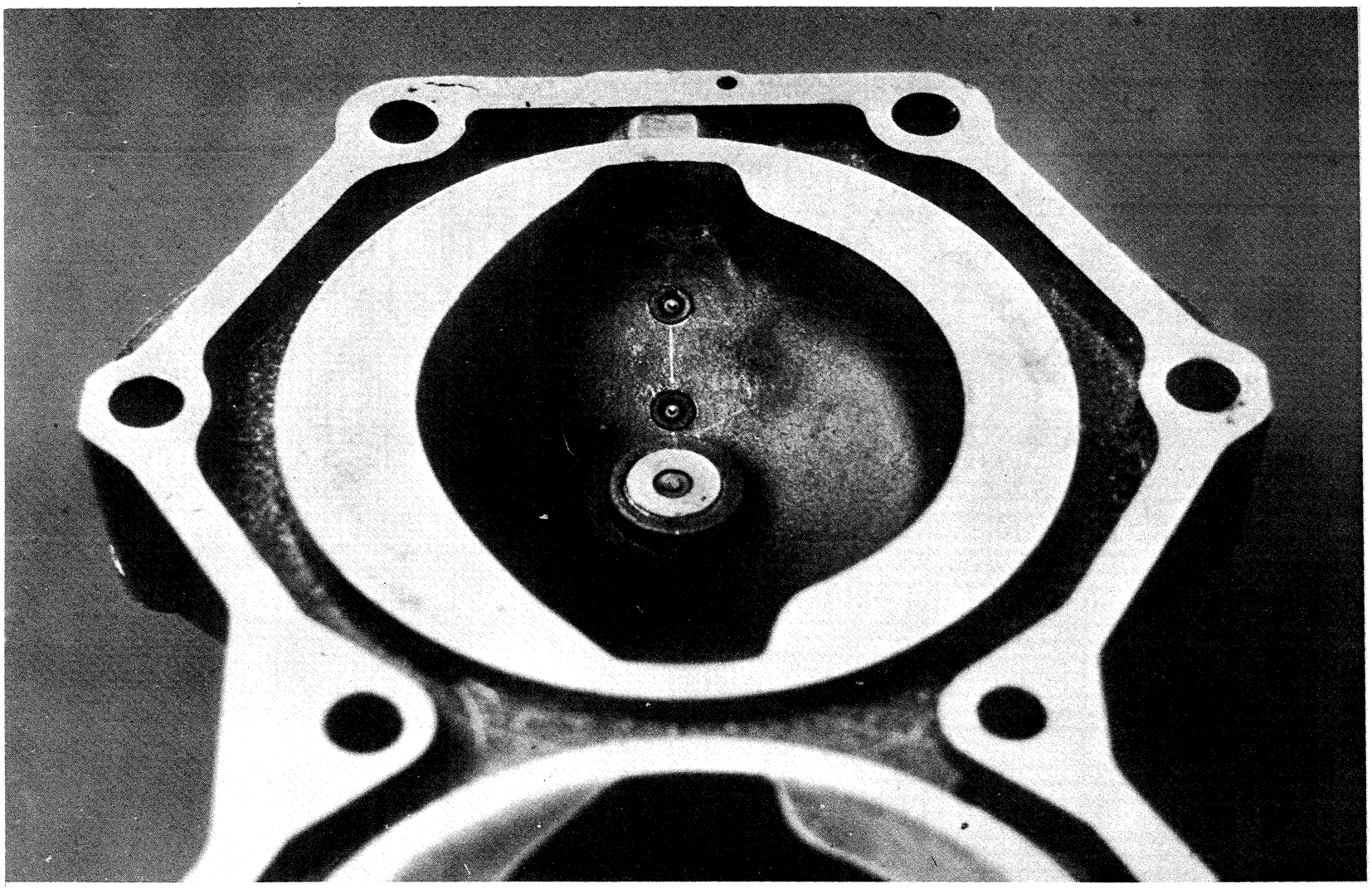

Figure 1. Multiple ionization probes installed in the engine cylinder head—viewed from the combustion chamber.

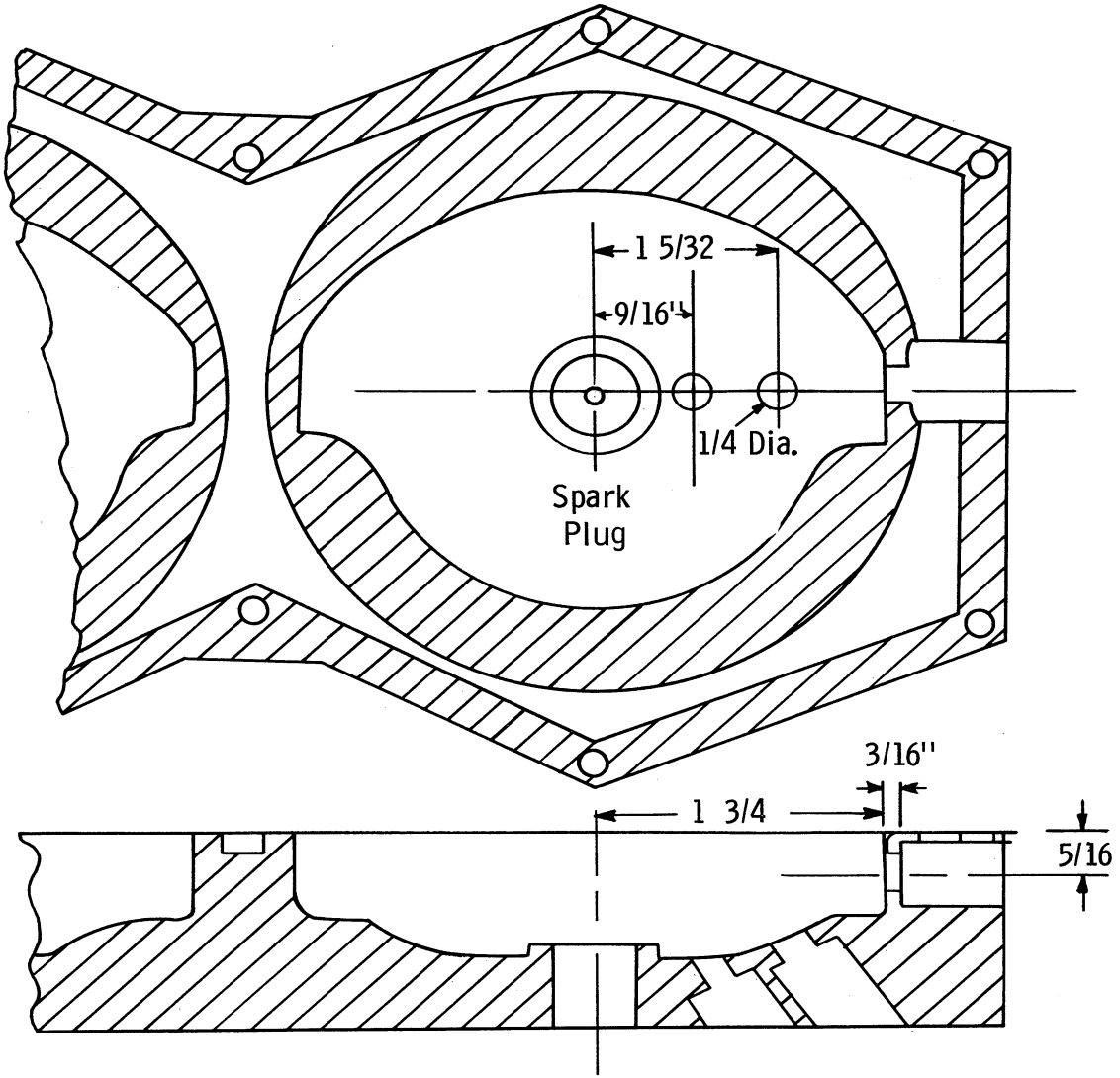

Figure 2. Schematic diagram of cylinder head with three mini-spark plug ionization probes.

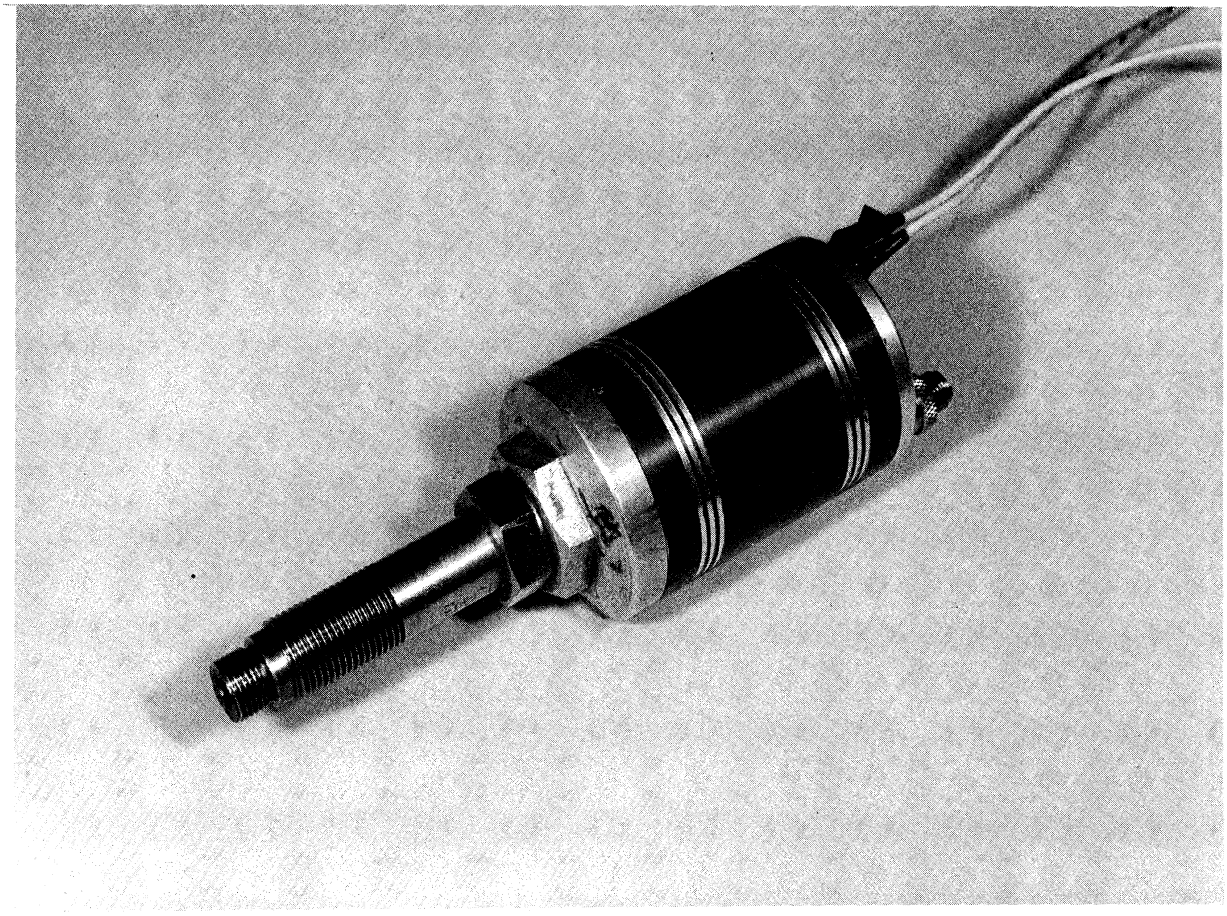

Figure 3. Cox electromagnetic sampling valve.

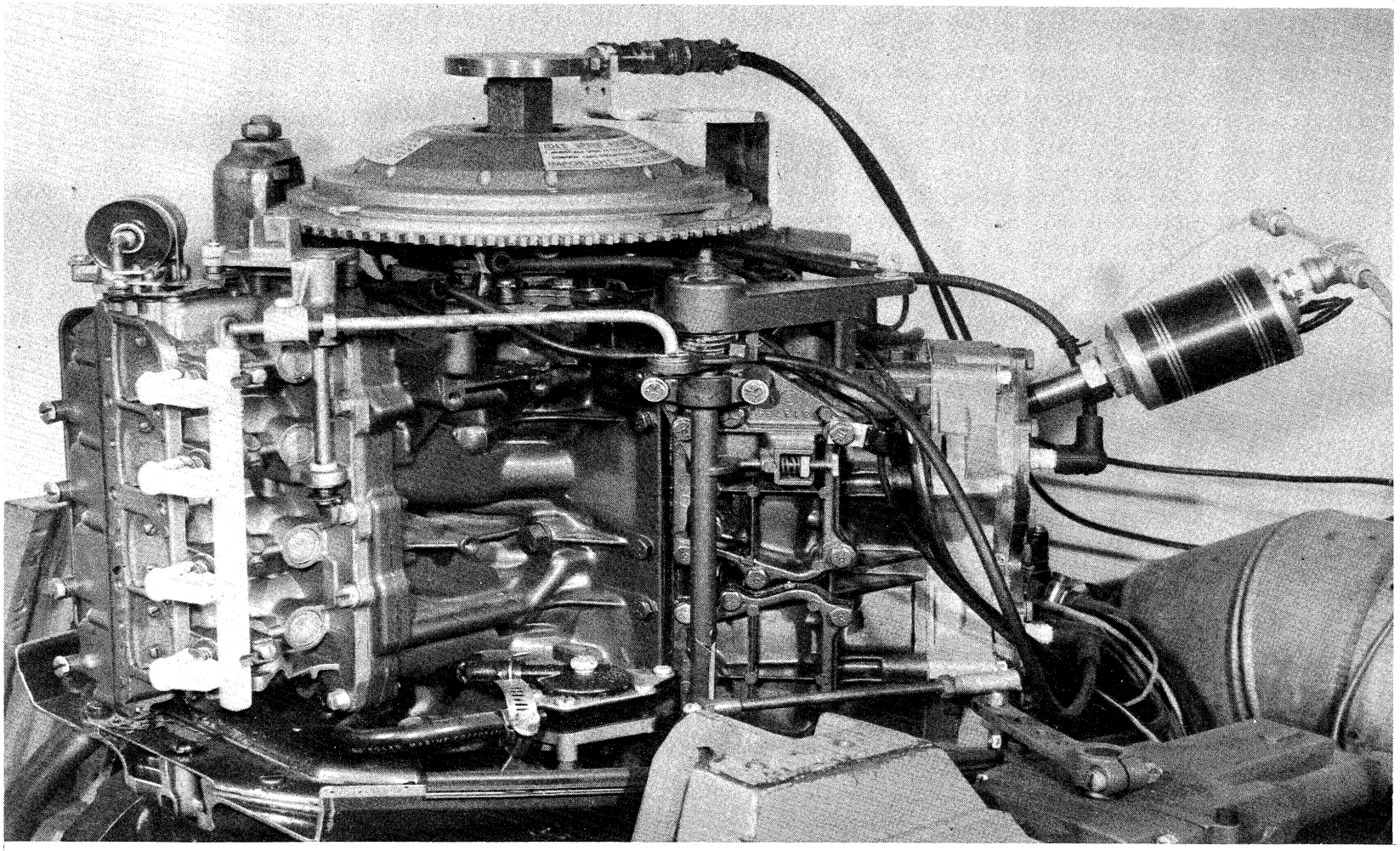

Figure 4. Cox sampling valve installed in the head of cylinder 2.

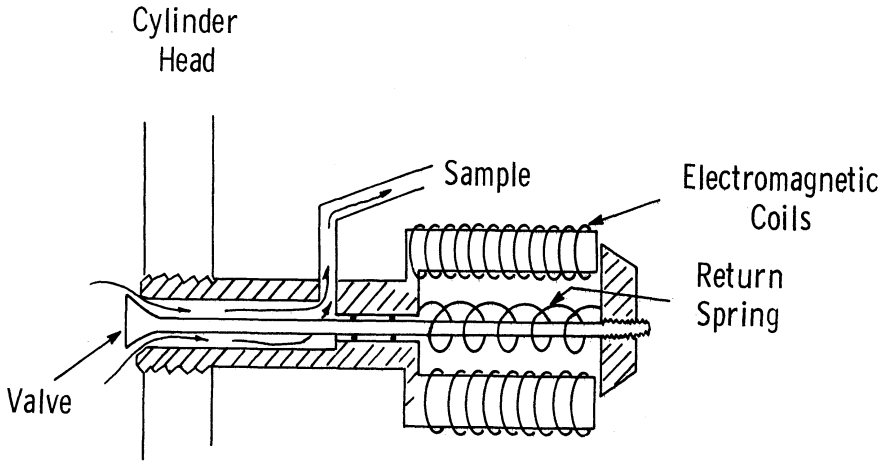

Figure 5. Schematic diagram of the Cox valve.

obtained. Duration of valve lift was found to be less than 10 msec. Because of low valve lift and relatively short duration of opening only a small sample was extracted from the cylinder. Even with critical flow, which existed during sampling, only a very small fraction of the cylinder charge was withdrawn and certainly did not affect the operation of the engine. The sample flow rate through the valve was very low, less than .5 cu ft per hr, cfh.

1. Control System

A small disc, tapped at 120° intervals, was attached to the flywheel. A steel stud placed in one of the three holes was used to generate an electrical signal when it passed through the magnetic field generated by the transducer. By utilizing this method, it was possible to place the magnetic pickup in a horizontal position, which eliminated interference from the signal generated by the magnetic cores in the flywheel. This system is shown schematically in Figure 6.

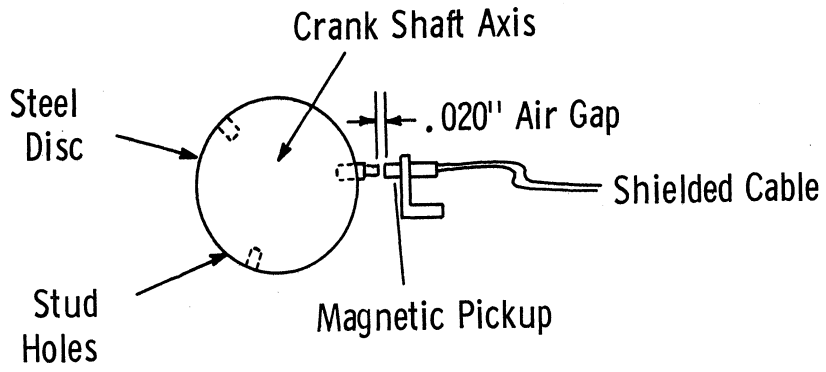

Figure 6. Trigger pulse system for actuating the Cox valve.

The sinusoidal signal generated by the magnetic pickup is used as an input signal to the control chassis. The circuit diagram of the electronic system used to drive the valve is shown in Figure 7. Pertinent circuit parameters are shown in Appendix A. The various waveforms generated are also illustrated on the wiring diagram as shown in Figure 7. Initially the pulse passes through a filtering circuit which, through the use of a zener diode, controls the amplitude of the signal. The signal is then directed to a dual gate circuit which functions as a Schmitt trigger. A square wave signal is now applied to a differentiating circuit converting the square wave to a positive-negative spike and then a diode eliminates the negative signal resulting in a single positive spike. The signal now passes through another similar delay circuit. Each delay circuit has three stages. The gate and RC network change the signal back to a square wave. By varying the resistance in the RC network, the duration of the square wave can be varied which in essence delays the signal. This wave is then passed through a gate arrangement which again sharpens the waveform, i.e., it squares the corners which were slightly rounded. This signal then passes through an additional differentiating circuit and changes the square wave back to a

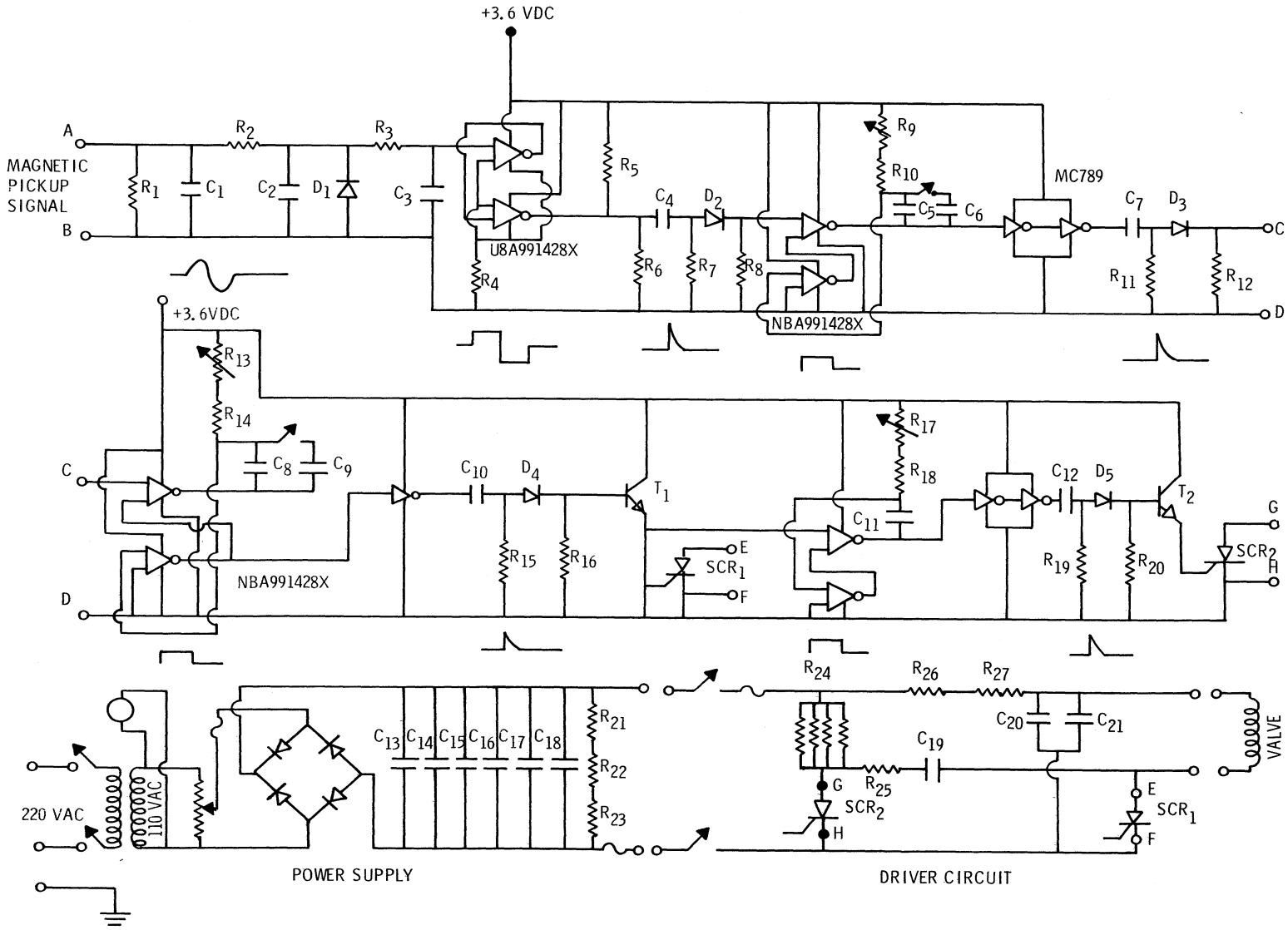

Figure 7. Circuit diagram—control circuit for the Cox valve.

positive spike. The second delay circuit operates in a similar manner; however, because of a difference in capacitance it functions as a coarse time delay. The signal is now conducted to the driver circuit. A 220 VDC power supply has charged up parallel capacitors which are in series with the poppet valve and a silicon controlled rectifier SCR. When the spike signal is applied to the gate of the SCR, it acts as a short circuit which allows the capacitors to discharge through the valve coils, momentarily popping the valve open. To cut off the SCR, the spike signal is sent through another delay circuit. It then triggers a second SCR which reverses the current flow through the first SCR and cuts it off.

The signal from the magnetic pickup was applied to one channel of a dual beam oscilliscope, and the driving spike to the other channel. By referencing the grid divisions on the scope to crank angle degrees, it was possible to adjust the valve opening to any crank angle.

Several problems were encountered with early system designs. The high rate of change of the engines ignition voltage (due to the C-D ignition system) generated an electro-magnetic field of sufficient strength to trigger the valve driver circuit when the circuit was located near the engine. To eliminate the electrical "noise," the control equipment was placed in an adjacent room and shielded cable was used for all exterior leads. Also a filter circuit was designed and included in the control box to eliminate any remaining electrical noise.

Engine velocity variations also caused problems, particularly at low speeds. The delay circuit triggering the poppet valve driver circuit operated

on real time. Cyclic variations of engine speed caused a variation in the crank angle of sampling, especially when the delay extended past 180°. To compensate for this, two additional positions for the triggering studs were added to the metal disc as shown previously in Figure 6. The delay was always less than 120° and this effectively controlled the variation. The single stud was placed in the hole preceding a given 120° range of sample collection.

2. Emission Instrumentation

After the sample was drawn from the cylinder it was ducted to the various emission instruments where the following constituents were analyzed:

CO
CO_2
Nondispersive infrared hydrocarbon, NDIR-HC
Flame Ionization total hydrocarbon, FID-HC
O_2

Several nondispersive infrared (NDIR) instruments were used. The CO concentration was measured with an Olson-Horiba Mexa 300 NDIR. A Mexa 200 Olson-Horiba NDIR was used for the CO_2 analysis. The Beckman 315 NDIR used previously in the OMC program was employed for HC measurement.

Oxygen concentration was obtained with the Beckman Model 715 polaragraphic analyzer.

Total HC's were determined with the Beckman Model 109A flame ionization detector (FID).

All NDIR analyzers and the polaragraphic O_2 analyzer were connected in series. The FID analyzer was connected in parallel with the other units. The general orientation of the analyzers is shown in the schematic diagram of Figure 8.

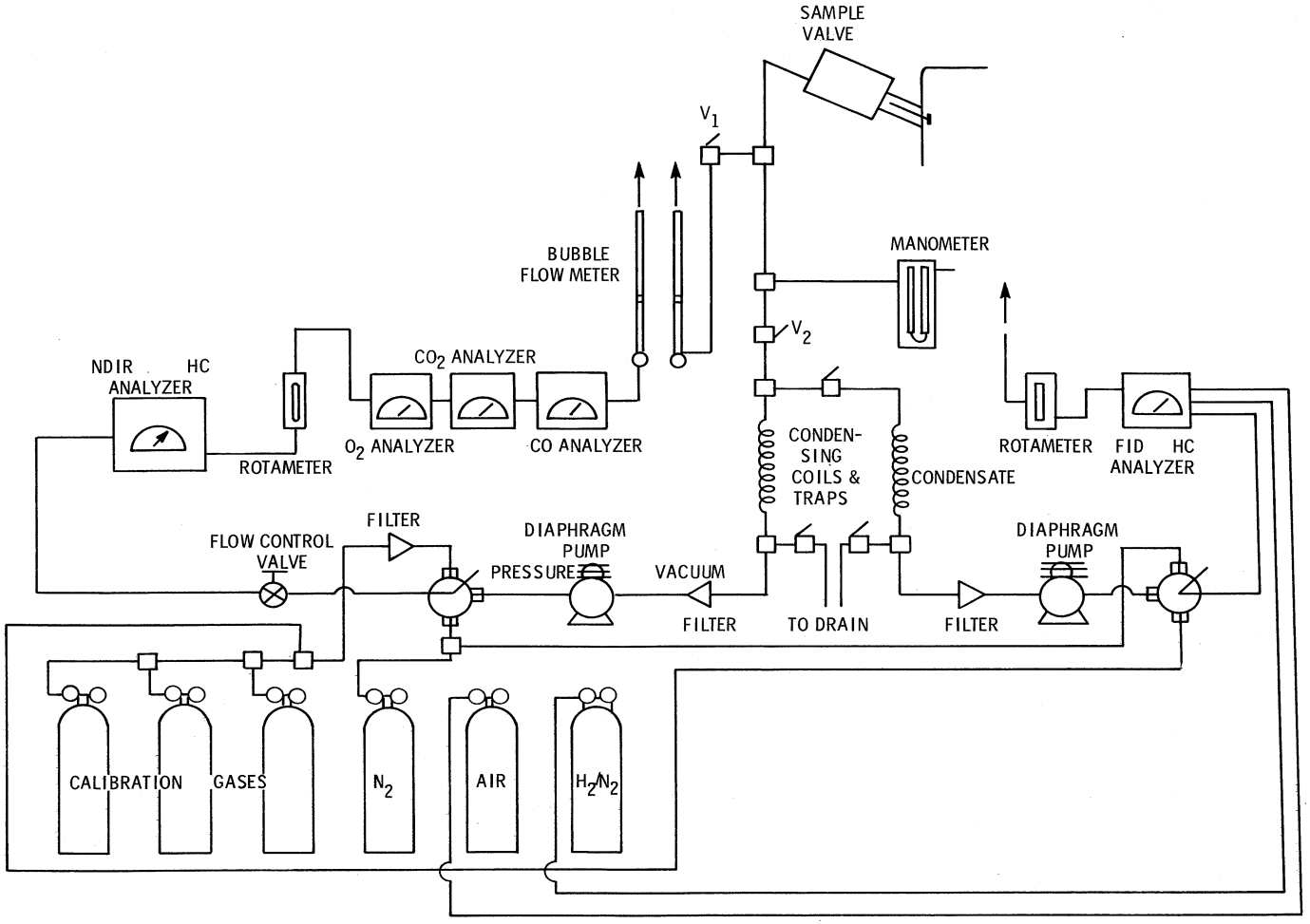

Figure 8. Schematic diagram—direct cylinder sampling gas analysis system.

A separate viton diaphragm pump was used to draw the sample into the NDIR instrumentation. The vacuum pumps built into the Olson-Horiba analyzers were disconnected and bypassed to facilitate effective flow control.

Since the sample flow rate was very low, $< .5$ cfh., the frequency response of the instrument train was long. To minimize this problem several changes were made in the system with the objective of decreasing the volume of the sample system. Where feasible, sample lines were shortened to a minimum and 1/4 in. tubing was replaced with 1/8 in. polyethylene tubing. Even with these modifications, the delay between sample induction at the Cox valve and the response of the analyzers was several minutes.

3. Sample System Leakage Analysis

Because of the severe effective restriction of the sampling valve, the sample line was operated substantially below atmospheric pressure. Consequently, the system was much more susceptible to outside air leakage and therefore dilution of the sample. To minimize this problem great care was taken in the assembly of the sample system. All unnecessary fittings were removed.

It is normally more difficult to detect leaks in a vacuum system than in a pressurized system because conventional "soap bubble" techniques are not applicable. A first stage leak check, however, was made by pressuring the lines and using the soap-water mixtures at all fittings. The second stage leak check was performed with the system under the operating vacuum conditions. A tee-connection was placed at the Cox valve—sample line junction. One branch was connected to a U-tube mercury manometer and the other to a nitrogen supply.

With the sample pump functioning, the N_2 regulator was adjusted to provide a system vacuum equivalent to operating conditions. Nitrogen should be the only constituent in the sample system unless, of course, an air leak is present. A leak is readily detected with the O_2 analyzer. A maximum O_2 concentration of .75% was observed which indicated a maximum leakage error of 3.5%. A secondary check was performed by connecting a calibration gas to the circuit at the sample line-valve junction. A reference gas of 8085 ppm n-hexane indicated 7750 ppm at the HC analyzer, a 4% error. The leakage error was less than the expected error of the instrumentation and was therefore neglected.

4. Sampling Valve Leakage Check

Another potentially serious source of experimental error was from a faulty sample valve. If the poppet valve failed to seat properly, leakage could occur and therefore result in a nonrepresentative sample being drawn into the analysis system. This error can be particularly serious if a constituent of low concentration is being analyzed from one interval of the cycle when the same constituent exists in a high concentration during another interval. For example, assume that CO_2 is being analyzed in the low pressure precombustion phase where its concentration is low. If the valve leaks during the complete engine cycle, the CO_2 reading will be markedly influenced by the region of the cycle (high pressure post-combustion), where the CO_2 exists in a much higher concentration.

A leakage check was regularly performed before and after each period of testing. The check was conducted by cycling values V_1 and V_2 (Figure 8) which

in essence connected the sample valve to a very sensitive bubble flow meter. With the engine operating and consequently a periodic high pressure applied to the valve even a minute leak would be detected by the flow meter. Fortunately, we did not detect any leakage problem that was not readily correctable in the range of the test. However, even if leakage had regularly occurred, this could have been corrected by using the following procedure.

Construct a graph of the concentration of the component of interest plotted as a function of the average static leakage rate measured with the bubble plot flow device. Refer to Figure 9 as an example of the technique. Over a number of test runs with varying leakage rates, a series of points will be located. By connecting these points a curve is defined which may be projected to a leak rate of zero. The value of the concentration measurement at zero leakage (A) is the data corrected for valve leakage.

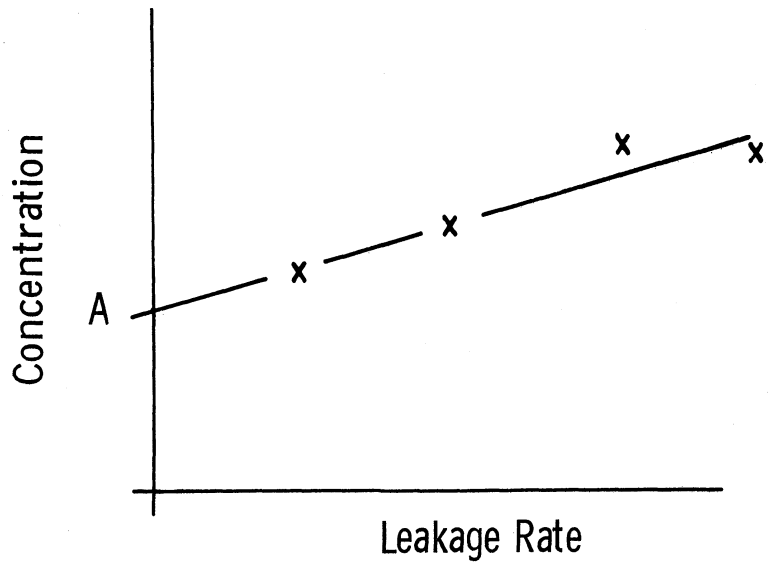

Figure 9. Technique for correction of sample valve data for leakage.

C. SCAVENGING SIMULATION

One of the most important components of the scavenging simulation was a single cylinder (Waukesha Fuel Research) 4-stroke cycle spark ignition engine. It was used as a high temperature gas generator providing nearly complete products of combustion (little incomplete burning was observed as evidenced by the low O_2 concentration. The hydrocarbons present in the exhaust were therefore primarily associated with the quenching process.) The following table lists specifications of the engine and its dynamometer. The exhaust gases were

TABLE I

SPECIFICATIONS OF THE SINGLE CYLINDER ENGINE—DYNAMOMETER

Engine—Waukesha Fuel Research—High Speed

Bore:	3.25 in.	
Stroke:	4.50 in.	
Displacement:	37.33 $in.^3$	
Spark ignition valve timing:	intake opens:	10° ATDC
	intake closes:	34° ABDC
	exhaust opens:	40° BBDC
	exhaust closes:	15° ATDC

Dynamometer—General Electric Type TLC 7.5

H.P. absorbtion:	15
Speed:	2000-4000 rpm

directed through an insulated manifold to a surge tank of approximately .2 cu ft. Figure 10 is a front view of the engine and FID hydrocarbon analyzer. The exhaust surge tank and fuel system is shown in Figure 11. Fuel for the single cylinder engine and simulation fuel/air mixture was distributed and measured with this apparatus.

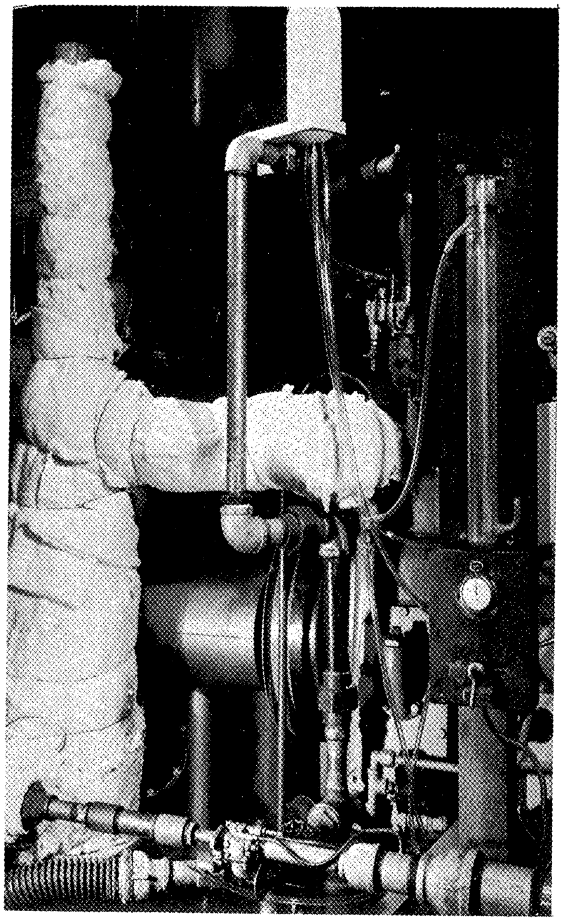

Figure 10. Front view of the single cylinder engine—scavenging simulation.

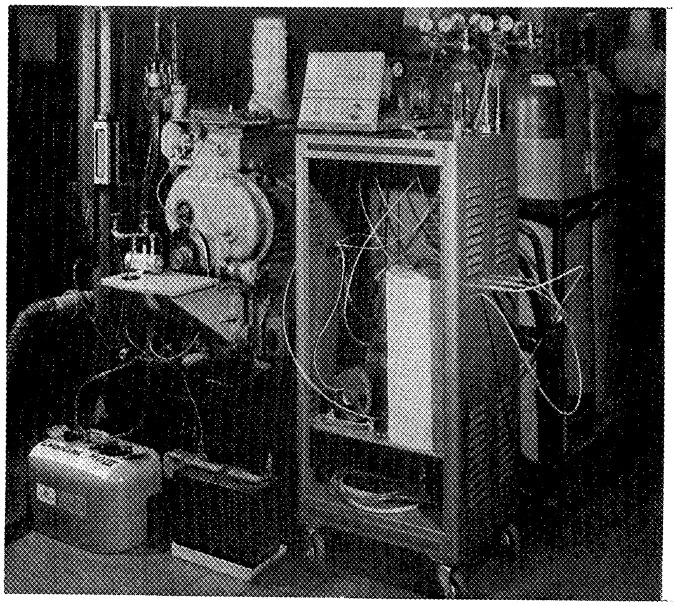

Figure 11. Side view of single cylinder engine, exhaust surge tank, and fuel control system—scavenging simulation.

At the exit of the surge tank the hot exhaust was directed into a mixing chamber where it was mixed with a carbureted fuel/air mixture. After complete mixing of the fuel and air with the hot exhaust it entered the reactor system which is the basic component of the scavenging simulation. The system is shown in the photograph of Figure 12 and schematically in Figure 13.

Stainless steel pipe of 1.5 in. I.D. was used for the reactor. Three static sample probes were installed in the reactor in the positions shown in Figure 12. Chromel-alumel thermocouples were positioned near each sample probe and at the inlet and outlet of the surge tank.

The auxiliary fuel/air mixture system, shown at the bottom of Figure 11 and schematically in Figure 13 was used to deliver an unburned mixture into the hot exhaust stream. A Johnson 2 HP outboard engine carburetor was the principal component of the system. Air was obtained from the high pressure shop supply but was regulated, controlled, and measured with a critical flow air meter built specifically for this purpose, Figure 14. Because the pressure in the carburetor air flow path was greater than atmospheric pressure, the carburetor was modified slightly by balancing the float bowl to the upstream pressure. The fuel/air ratio was controlled with the adjustable needle valve. Fuel rate was measured with the precision rotometer shown at the left of the engine in Figure 10.

A flame arrestor was incorporated in the pipe connecting the carburetor to the mixing volume to prevent the possibility of backfiring. A schematic of the mixing volume is shown in Figure 15. It was designed similar to the gas mixer used by Sorenson (Ref. 4).

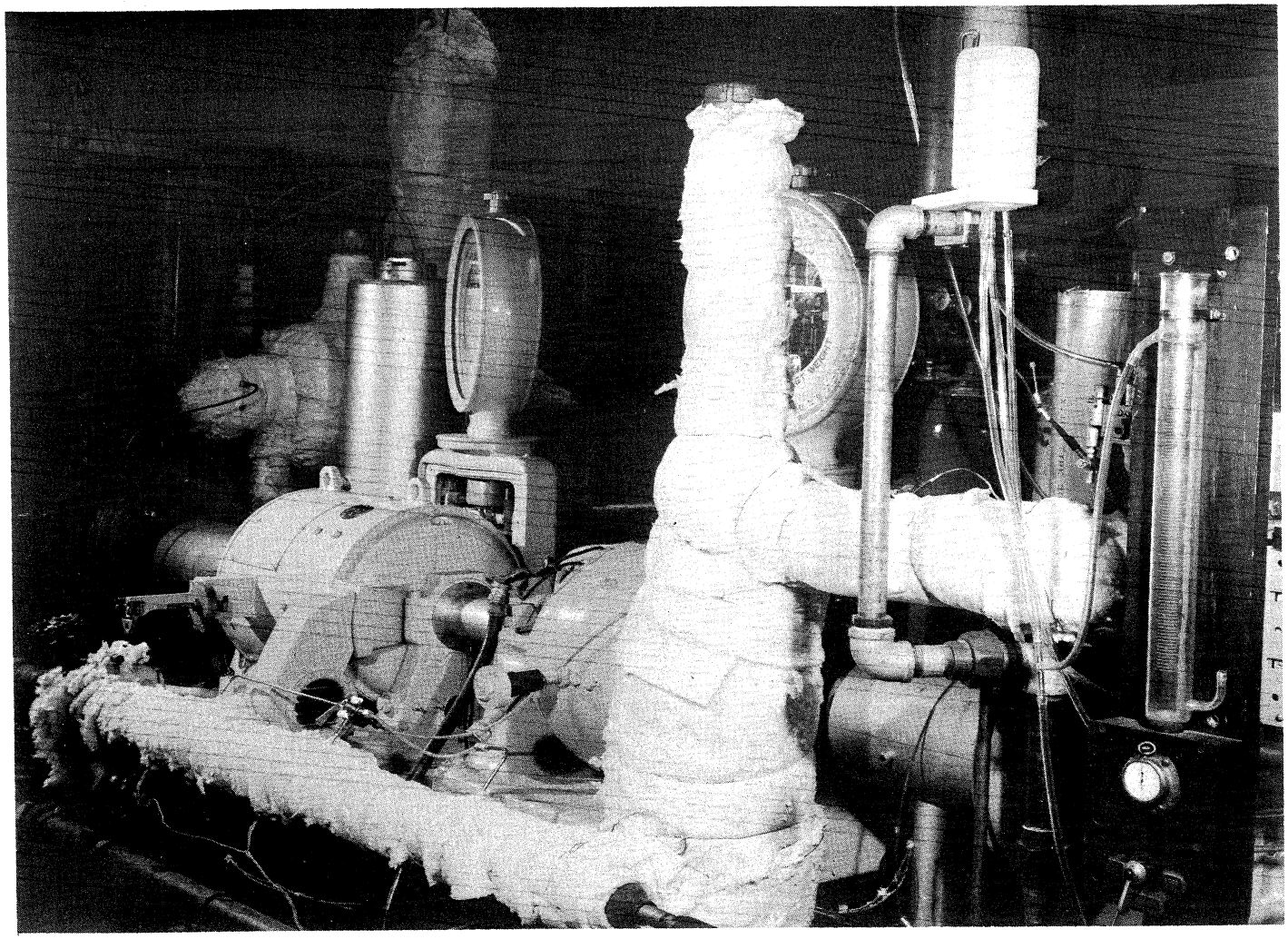

Figure 12. Scavenging simulation reaction chamber.

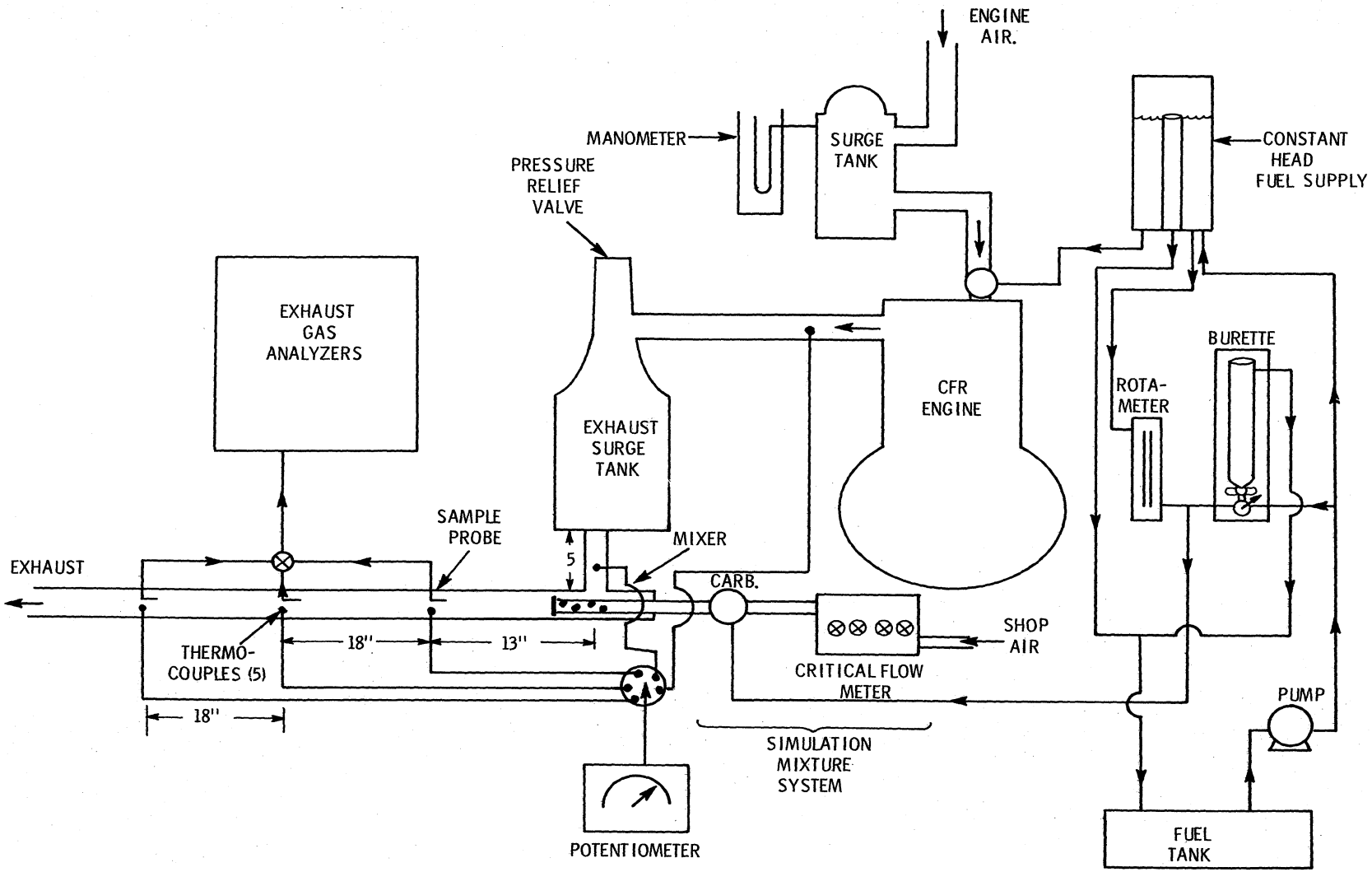

Figure 13. Schematic diagram—scavenging simulation.

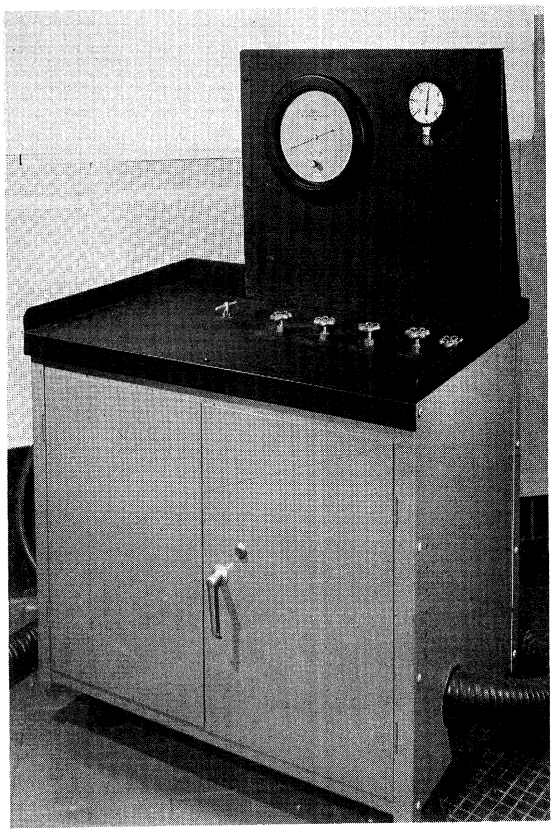

Figure 14. Critical flow air meter.

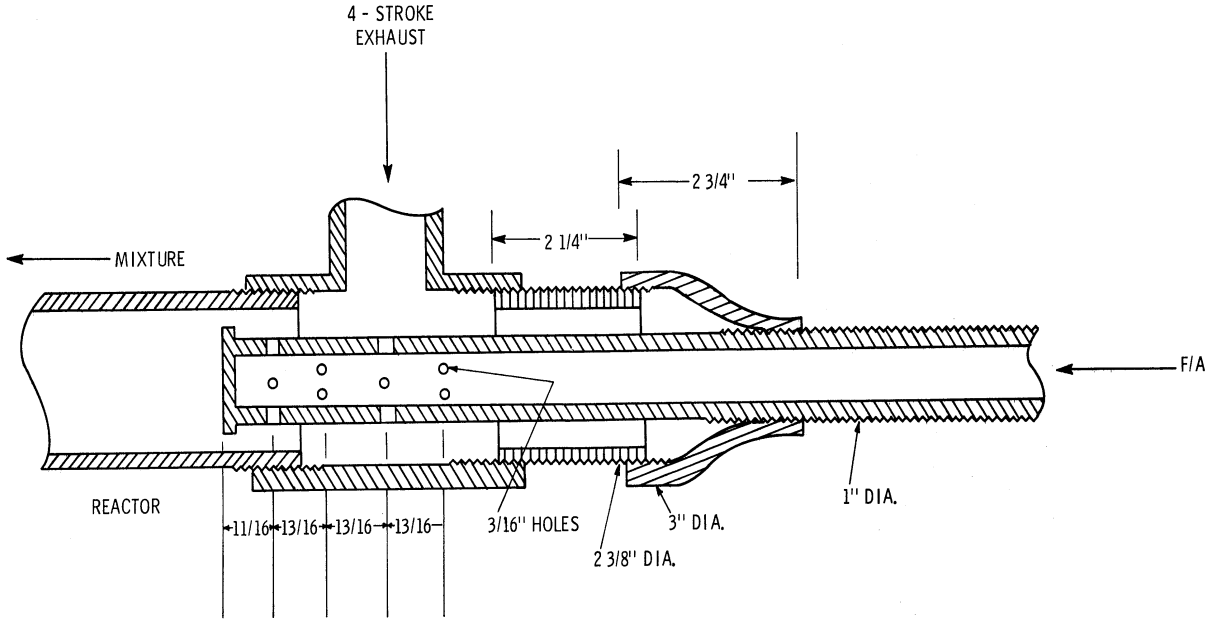

Figure 15. Schematic diagram—fuel-air mixture and exhaust gas mixing system.

The complete high temperature system was insulated with several inches of Babcock and Wilcox "Kaowool" ceramic fibre. With this insulation and the engine adjusted for maximum exhaust gas temperature, temperatures of 1270°F were attained in the reactor without fuel/air mixture addition and 1130°F with the mixture added. Under steady state conditions and no mixture addition, a temperature difference of 100°F was observed from probe 1 to probe 3. This was caused by some heat transfer from the reactor. A more detailed discussion of the temperature environment is presented in the results section.

1. Instrumentation

The primary exhaust species of interest were the unburned hydrocarbons. A Beckman Model 109A flame ionization detector was used in conjunction with a subtractive column analyzer (Ref. 5) to detect total HC as well as the major HC families (paraffins, aromatics, and olefins).

The subtractive column analyzer is shown schematically in Figure 16 and in the photograph, Figure 17. Basically the sample is directed alternately to the packed columns or scrubbers. An automatic cycling timer is incorporated to regulate and control the time of flow in the scrubbers. The timer operates solenoid valves that divert the sample flow through a single scrubbing system, while the scrubbers not in use are maintained in a "backflush" condition to purge any incompletely absorbed materials.

The University of Michigan subtractive column unit was checked against a gas chromatograph, Beckman GC-4, at the Ford Motor Company Engineering Staff. The tests were run using exhaust from an idling 2000 cc Pinto. Three series of tests were run.

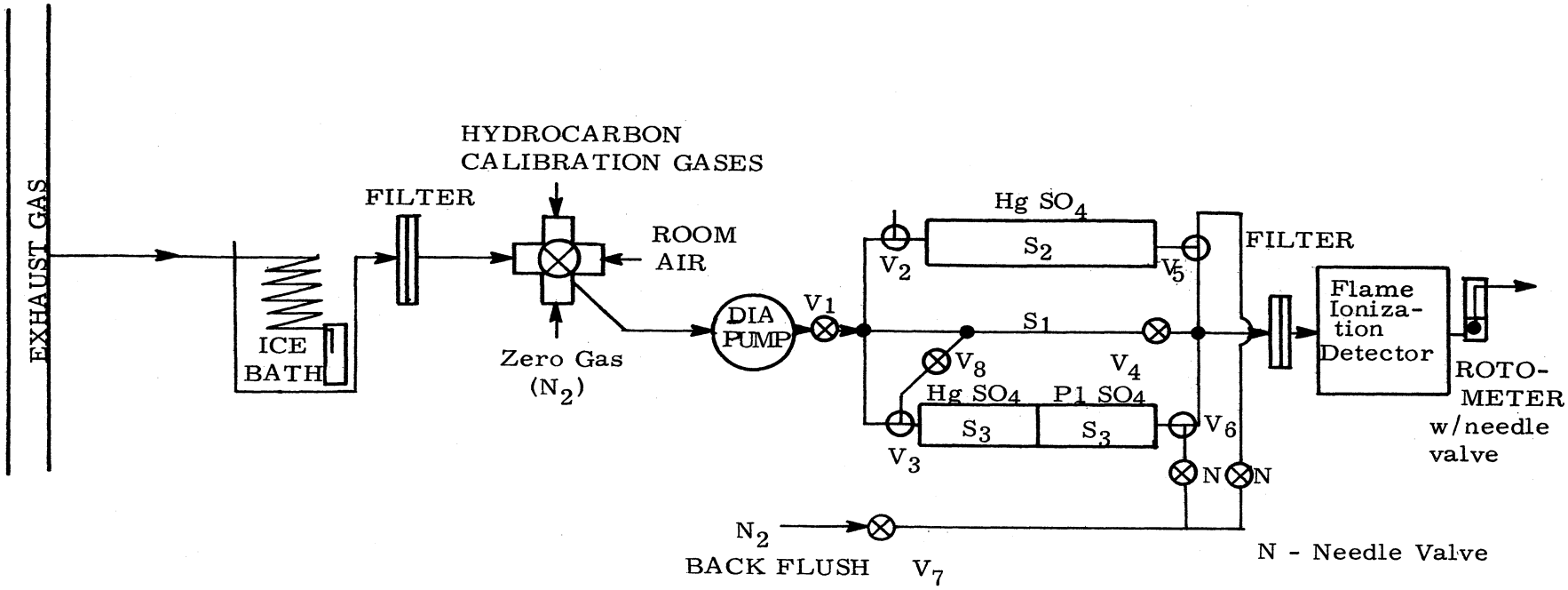

Position	Sample Seen by FID	Flow Path	Scrubber	Operation of Valves $V_{7,8}$	V_1	$V_{2,5}$	$V_{3,6}$	V_4
1	Back flush	S_2S_3	All	On	Off	Off	Off	On
2	Paraffins and benzene	S_3	$HgSO_4$ and Pd	Off	On	Off	On	Off
3	Total olefins	S_2	$HgSO_4$	Off	On	On	Off	Off
4	Total or zero	S_1	None	Off	On	Off	Off	On

Figure 16. Flow schematic of the University of Michigan subtractive column—flame ionization hydrocarbon analysis system.

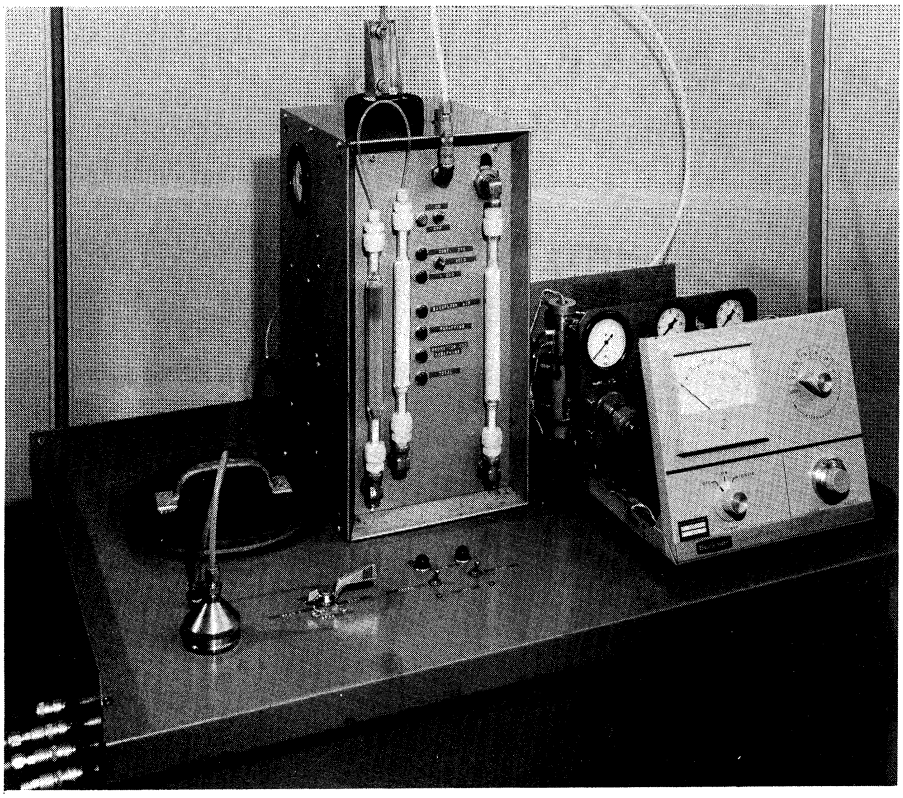

Figure 17. The University of Michigan subtractive column—flame ionization hydrocarbon analysis system.

In the first test, exhaust was passed through the olefin + aromatic subtractor columns and then to the G.C. The following results were obtained (ppmc):

Paraffins	Olefins & Acetylenes	Aromatics	Total
1087	19	44	1150

The analyzer would report 1150 ppmc as paraffins rather than the correct 1087. Thus the error in reporting paraffins was +63/1087 or +5.8%. Our analyzer overestimated the paraffin content of the exhaust by 5.8%.

In the second test additional exhaust gas was passed through the olefin subtractor only. The results were:

Paraffins	Olefins & Acetylenes	Aromatics	Total
1344	27	1130	2501

The analyzer would report 2501 ppmc as paraffins and aromatics rather than the correct 2474. Thus the error in reporting paraffins plus aromatics was +27/2474 or +1.1%. The error in reporting aromatics alone must be estimated since the emission base line shifted between tests. If it is assumed that the subtractive column would report paraffins 5.8% too high, then an estimated value would be: 1344 x 1.058 = 1420 ppmc. By differencing, we find 2501 - 1420 = 1081 to be the aromatic content that would be reported by the subtractive column. The error is 1130 - 1081 or 49 ppmc. Thus the subtractive column underestimated aromatics by 49 ppmc or -49/1130 = -4.3%.

In the final test, exhaust was passed directly into the G.C. The results were:

Paraffins	Olefins & Acetylenes	Aromatics	Total
1364	1905	1453	4722

In the above test paraffins plus aromatics were 2817 ppmc. From Test 2, this may be assumed to be 1.1% lower than the subtractive column would yield. The subtractive column value would be 2817 x 1.011 = 2848 ppmc. The subtractive column prediction of olefins plus acetylenes would then be 4722 - 2848 = 1874. This is too low by 1905 - 1874 = 31 ppmc or -31/1905 = -1.6%.

Based on these G.C. results one can conclude that the subtractive column class results differed from G.C. class results as shown below:

Class	Percent Error
Acetylenes + olefins	-1.6
Aromatics	-4.3
Paraffins	+5.8

Since acetylenes were about 7.5% of the total in these tests, interpreting the subtractive column results to be olefins rather than olefins plus acetylenes would overestimate olefin content by 5.8%.

Considering the nonparaffin constituents which broke through in Test 1, 14 were olefins and 6 aromatics. Of the 14 olefins, 7 were either 2 or 3 ppmc, the rest were less. Of the 6 aromatics, the ppmc contributions were:

Constituent	ppmc after Subtraction
Benzene	3
Toluene	17
Ethyl benzene	5
Xylenes	6
Mono substituted ethyl benzenes	8
Die substituted ethyl benzene	5
Total	44

Only 1 or 2% of the smaller aromatics broke through but virtually all of the large aromatics did. This result is different from that of Sigsby. In his tests virtually no larger aromatics broke through but a large percentage (> 80%) of benzene did. Fortunately the concentration of the larger aromatics is small.

In conclusion, within the limitations of test with shifting baseline emission levels, the subtractive columns were very accurate (better than 6%) in reporting the classes. The major drawback is that acetylene is reported as an olefin.

In addition to the HC analysis, CO, CO_2, O_2 were monitored with the instrumentation discussed previously. This additional data was particularly useful for measuring fuel/air ratio as well as measuring oxidation reaction of the unburned fuel.

III. RESULTS AND ANALYSES

A. SCAVENGING SIMULATION

Development of an effective scavenging simulation is still underway. The initial program was perhaps overly ambitious with the following parameters proposed as independent test variables.

1. Trapping efficiency - Γ
2. Fuel/air ratio
3. Fuel type
4. Reactor temperature

The objective of this program was to determine the influence of these parameters on the total and family hydrocarbon concentration in the simulated scavenged mixture as a function of the reactor residence time.

Numerous problems have been encountered in the test program to date and have resulted in modification of the original objective. Rather than using a large combination of the before mentioned parameters, the trapping efficiency, fuel/air ratio and reactor temperature profile are held constant while varying the fuel type. This should provide a clue to the chemical history of the through scavenged fuel as it becomes an exhaust emission.

1. Mixture Residence Time

Several basic calculations were performed to insure that the gas residence time in the simulation was approximately the same as in the engine. At the lowest tested engine air and fuel flow rates (1000 rpm boat load condition),

residence time of the unburned mixture is the greatest. If residence time is the key parameter controlling the decomposition of the fuel, it is the most critical test condition. However, if exhaust gas temperature is the most influential variable, the higher engine speed and load conditions may result in the greater fuel decomposition even with the decreased residence time. It is possible to gain some inference to the reaction by examining a basic kinetic expression for the oxidation of hydrocarbons in a thermal reactor. Eltinge, et al. (Ref. 6) presented the following relationship

$$C_o = C_i \, e^{-\frac{K_r P^2 O_2 V}{K_3 T^2 W}}$$

where

C_o = concentration of hydrocarbons in the exhaust gases leaving the reaction volume, ppm (vol)

C_i = concentration of hydrocarbons in the exhaust gases entering the reaction volume, ppm (vol)

e = base of natural logarithms

P = exhaust pressure, psia

O_2 = oxygen concentration in the exhaust gases, % (vol)

V = volume available for exhaust gas reaction, ft^3

T = absolute temperature, °R

W = mass flow rate of air, lb sec^{-1}

K_3 = numerical constant

K_r = specific reaction rate, ft^3 lb-mol^{-1} sec^{-1}

The exponential term is the fraction unreacted; if the combination of oxygen, pressure, temperature, and time is insufficient, its argument approaches zero and its value approaches 1.0. The expression shows that the factors have interrelated effects and is a useful aid in understanding the thermal decomposition of the hydrocarbons. Reaction rate is strongly dependent on temperature. The increase in specific reaction rate, K_r, far outweighs the effects of reduced densities reflected in the T^2 term and the other factors including residence time. This strongly suggests that the most influential parameter governing the HC decomposition in the unburned 2-cycle charge is temperature.

To assess the relative importance of the several parameters in the 2-cycle engine, residence time was approximated and exhaust temperature measured for the 100 hp engine. Several assumptions were made including:

1. Flow system behaved essentially as a plugflow reactor; therefore, the time and spatial coordinates could be interchanged.
2. Measured exhaust temperature was the average temperature to which the unburned fuel was exposed.
3. Volume of gases exposed to the high temperature environment was two times the individual cylinder volume, V = 50 cu in.
4. Pressure during scavenging was atmospheric, P = 14.7 lb/in.^{2}
5. Gas constant was approximated by that of air, R = 53.35 ft lbf/lbm°R.

Because the qualitative trend of decomposition was sought, minor errors implicit in these assumptions were not believed to be of major importance. The approximate density of the scavenged mixture and exhaust gases was computed from the perfect gas relationship.

$$\rho = \frac{P}{RT}$$

Pertinent engine data and calculations are summarized in Table II.

TABLE II

ENGINE ASSUMPTIONS FOR SCAVENGING SIMULATION

Boat Load rpm	Exhaust Port Temp. °F	Engine* Mass Flow lb/hr	Mass Flow per Cylinder lb/hr	Scavenged Volume per Cylinder	Density lb/ft^2	Residence** Time sec
1000	600	21	5.25	50 $in.^{-3}$	.0375	.74
2000	850	155	38.9	50 $in.^{-3}$	.0302	.081
3000	1000	275	69	50 $in.^{-3}$	.0272	.042
4000	1150	535	134	50 $in.^{-3}$	.0246	.019

*Engine mass flow is the sum of air and fuel flow rate in the 100 HP engine.
**Residence time assuming plug flow.

2. Reactor Sizing

The reactor volume of the simulator was approximated for the 2000 rpm test condition, $t_{residence}$ = .081 sec., ρ = .0302 $lb/ft.^3$ The single cylinder engine flow rate was 43 lb/hr and the simulated trapping efficiency was assumed to be .75 for these calculations. Hence the total reactor flow was 57.3 lb/hr. The engine could be throttled to decrease the flow rate necessary to achieve the long residence time observed at the 1000 rpm test condition. Required reactor volume, V_r, was calculated from the following expression:

$$V_r = \frac{\dot{V}}{\rho} t_R$$

where

$\dot{V}$ = volume flow rate = $43/\Gamma$

t_R = residence time

ρ = gas density

$$V_r = \frac{57.3 \text{ lb/hr}}{.0302 \text{ lb/ft}^3} \times \frac{.081 \text{ sec}}{3600 \text{ sec/hr}} \times \frac{1728 \text{ in.}^3}{\text{ft}^3} = 73 \text{ in.}^3$$

To satisfy this requirement a reactor of 1.5 in. inside diameter and 5 ft length was used in the apparatus (V_r = 106 in.^{3}).

By either changing the position of the exhaust sample probes or the single cylinder engine air rate, the residence times of the other test conditions could be simulated quite accurately.

3. Reactor Temperature Profile

The spatial temperature distribution was an important consideration in the reactor. With the single cylinder engine operating with 10° spark retard, a maximum temperature of 1550°F and 1400°F were observed at the engine exhaust port and surge tank exit respectively, Figure 18. The reactor temperatures are also shown in Figure 18 for three different test conditions; engine exhaust only, Case I, engine exhaust plus 25% air ($\Gamma = .75$) Case II, exhaust plus 25% air-fuel mixture added ($\Gamma = .75$) Case III. As expected, the system with the exhaust only operated somewhat hotter than the other conditions, particularly at sample probe 1. However, the temperature dropped moderately along the reactor with the pure exhaust. This temperature drop was expected because of some heat transfer along the length of the reactor even though it was well insulated. A uniform temperature profile could be obtained only if the reactor were externally heated.

When air was added to the system, Case II, the temperature at probe 1 decreased by approximately 60°F, because of dilution of the hot exhaust with

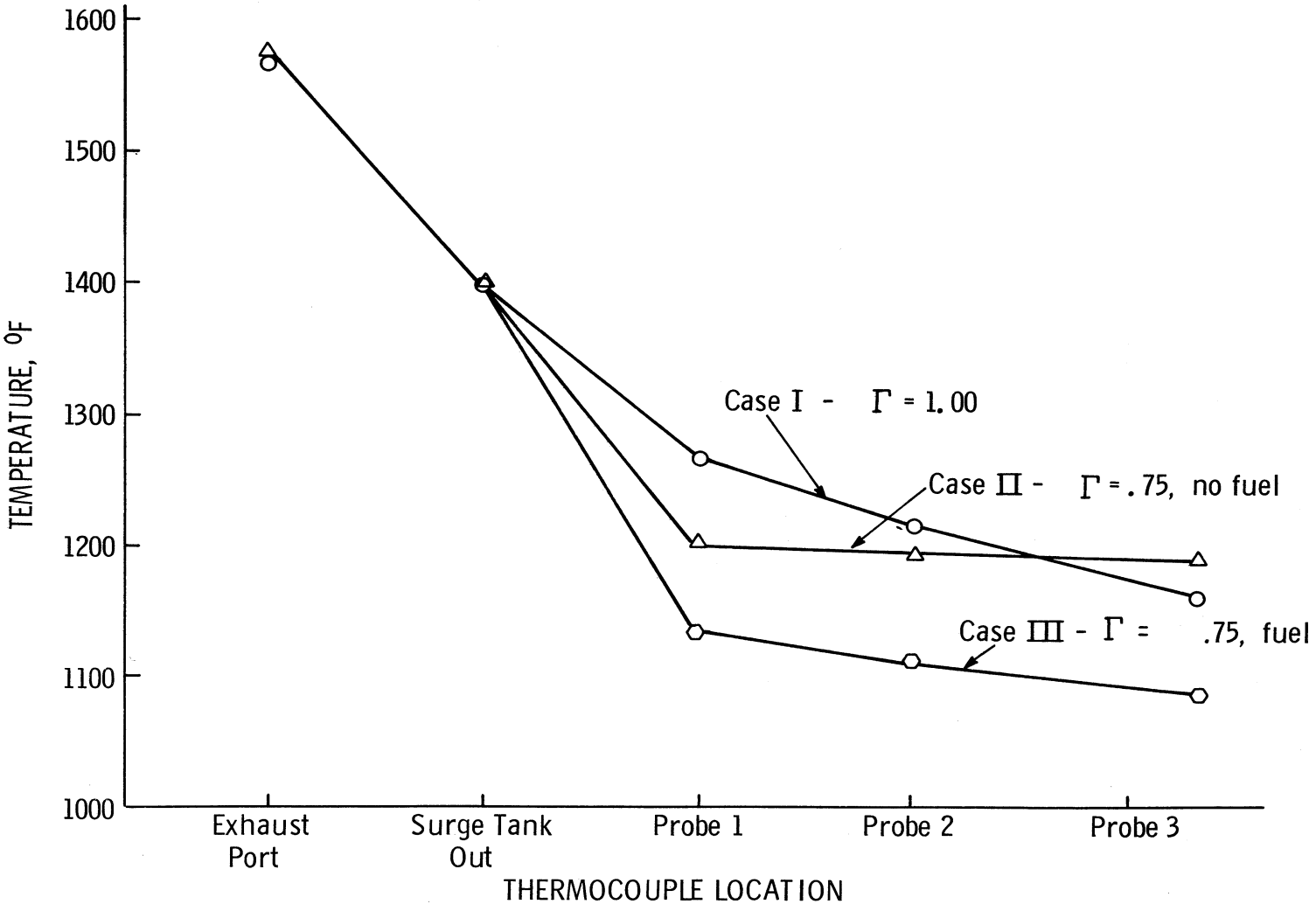

Figure 18. Exhaust pipe and reactor temperature profile.

the relatively cool air. It was interesting to note that the temperature remained nearly constant along the reactor and, in fact, was greater at probe 3 than observed in the previous case. Apparently the added air was partially reacting with combustibles in the engine exhaust with the heat release being approximately equal to the heat loss from the reactor surface.

When the air and fuel mixture (A/F = 14/1) was added to the hot exhaust in the mixer, Case III, the temperature decreased moderately from the prior case. The temperature decreased along the reactor by approximately 40°F from probe 1 to probe 3. This temperature decrease suggests that the added fuel is not reacting significantly along the reactor. The temperature drop can be attributed to the cooling effect of the fuel because of its relatively high heat of vaporization. For this case, which is the one of importance in the simulation, the temperature history was comparable to the temperatures measured in the 100 hp engine exhaust at 4000 rpm. With higher simulated trapping efficiencies the temperature would be lowered in proportion to the fraction of mixture added.

Generally the reactor does appear to offer a temperature environment similar to the engine if the basic assumptions are accepted. The unburned fuel chemistry should be at least qualitatively similar to that of the real engines over scavenged fuel.

From a relatively simple thermal analysis of the reactor, it appears that the fuel experiences only a very limited reaction. And, the initial test condition used in the "shakedown" study is substantially more rigorous than predicted for the 100 hp, 2-cycle engine. The residence time is similar to

the 2000 rpm operating condition and temperature history similar to the 4000 rpm condition. The analytical procedure is quite simple and basically consists of comparing the energy release from burning in the reactor with heat transfer from the reactor.

Case I—in the simulator without the addition of the fuel mixture, the heat loss is calculated to be approximately 1080 Btu with the following test conditions and assumptions:

1. $\Delta T_{\text{probe 1-3}} = 105°F$
2. Mass flow = 43 lb/hr
3. Specific heat = .24 Btu/lb°F
4. No chemical reaction—with the rich mixture used in the single cylinder engine, little O_2 is available for reaction in the exhaust

Case III—with the addition of the fuel/air mixture, the heat loss between probes 1 and 3 was approximately 560 Btu/hr, with a slight increase in total reactor flow rate, 53.7 lb/hr, and a decrease in ΔT to 45°F.

It therefore appears that, as a maximum, no more than 1080 - 560 = 520 Btu/hr could have been released from an exothermic reaction of the fuel. With a fuel/air scavenging mixture of 13/1, the total fuel rate (unburned mixture) was .78 lb/hr. Assuming a heating value of 20,000 Btu/lb, the maximum heat release with complete burning would be approximately 15,000 Btu/hr. Certainly even if the 520 Btu/hr energy were derived from fuel combustion, the reaction was minimal (3-1/2% reaction).

A number of factors lead one to conclude that the actual degree of fuel reaction was much less.

1. No consideration was given to CO oxidation with the added mixture. Examination of Case II, air only added, revealed that the CO reaction may be significant and is the probable source of most of the energy release in Case II. Also thermal reactor studies on 4-cycle engines indicate that the CO reacts more readily than the exhaust hydrocarbons.

2. The temperatures were lower in Case III which would cause the heat losses to be somewhat less. However, this may have been partially counteracted by a slight increase in convective heat transfer coefficient due to higher flow velocities, and decreased time for heat loss because of the greater flow rate.

In any event, the thermal analysis of the reaction suggests that the fuel is engaged in only a minute exothermic-chemical reaction. However, some fuel decomposition reactions may be occurring with little energy release. Future analysis of aldehydes in the simulator should reveal the extent of these reactions.

4. Preliminary Reactor Gas Analysis Study

Substantial preliminary testing was conducted to assess the composition change of the fuel-air mixture along the reactor flow path, Case III, as discussed previously. Also as a basis for comparison the 4-stroke exhaust alone, Case I, and with air but no fuel added in the mixing section, Case II, were carefully analyzed.

Indolene HOIII, an unleaded reference gasoline blended by the American Oil Company, was used in this phase of testing. The composition of Indolene is much more carefully controlled than conventional gasoline. The approximate hydrocarbon family composition together with other pertinent data for Indolene

is shown in Table III.*

TABLE III

GENERAL RANGE OF SPECIFICATIONS OF
CLEAR INDOLENE—HOIII

		Typical Test Fuel
Composition		
Olefins (%)	10 max	4%
Aromatic (%)	35 max	30%
Saturates (%)	remainder	66%
Distillation		
Initial boiling point	75-95°F	
10% evaporation	120-135°F	
50% evaporation	200-230°F	
90% evaporation	300-325°F	
Maximum	415°F	
Hydrogen/Carbon Ratio	1.83	
API Gravity	59.0	

Preliminary gas analysis data is shown in Table IV and includes a HC composition breakdown of the important HC families. Data is presented for all three cases. The total HC concentration is plotted as a function of location in the reactor in Figure 19, and total HC, normalized to the results at probe 1, are shown in Figure 20. The uncorrected HC species fraction of paraffins, olefins, and aromatics is plotted in Figures 21,22, and 23 for the three different test conditions.

*In the final stage of the test program, the Indolene will be subjected to a more detailed HC family analysis.

TABLE IV

EMISSION RESULTS—TWO-CYCLE SCAVENGING SIMULATION

	Probe		
	1	2	3
Case I. Γ = 1.0, 4-cycle exhaust only			
CO (%)	5.8	5.8	5.7
CO_2 (%)	10.7	10.7	10.9
O_2 (%)	.2	.15	.15
Paraffins, ppm	230	240	240
Aromatics, ppm	230	250	250
Olefins, ppm	460	435	410
Total HC (C_6H_{14})	920	925	900
% Paraffins	25	26	27
% Aromatics	25	27	28
% Olefins	50	47	45
Case II. Γ = .75, air only added			
CO (%)	4.9	4.5	4.3
CO_2 (%)	8.8	8	8.4
O_2 (%)	3.7	4.8	4.9
Paraffins, ppm	190	170	160
Aromatics, ppm	180	180	150
Olefins, ppm	350	330	290
Total HC (C_6H_{14})	720	680	600
% Paraffins	26	25	27
% Aromatics	25	26	25
% Olefins	49	49	48
Case III. Γ = .75, fuel and air added			
CO (%)	3.7	3.5	4.1
CO_2 (%)	9.8	8.9	8.6
O_2 (%)	3.4	4.7	4.5
Paraffins, ppm	4800	5700	5600
Aromatics, ppm	1600	2100	2400
Olefins, ppm	800	1100	1000
Total HC (C_6H_{14})	7200	8900	9000
% Paraffins	67	64	62
% Aromatics	22	23	27
% Olefins	11	13	11

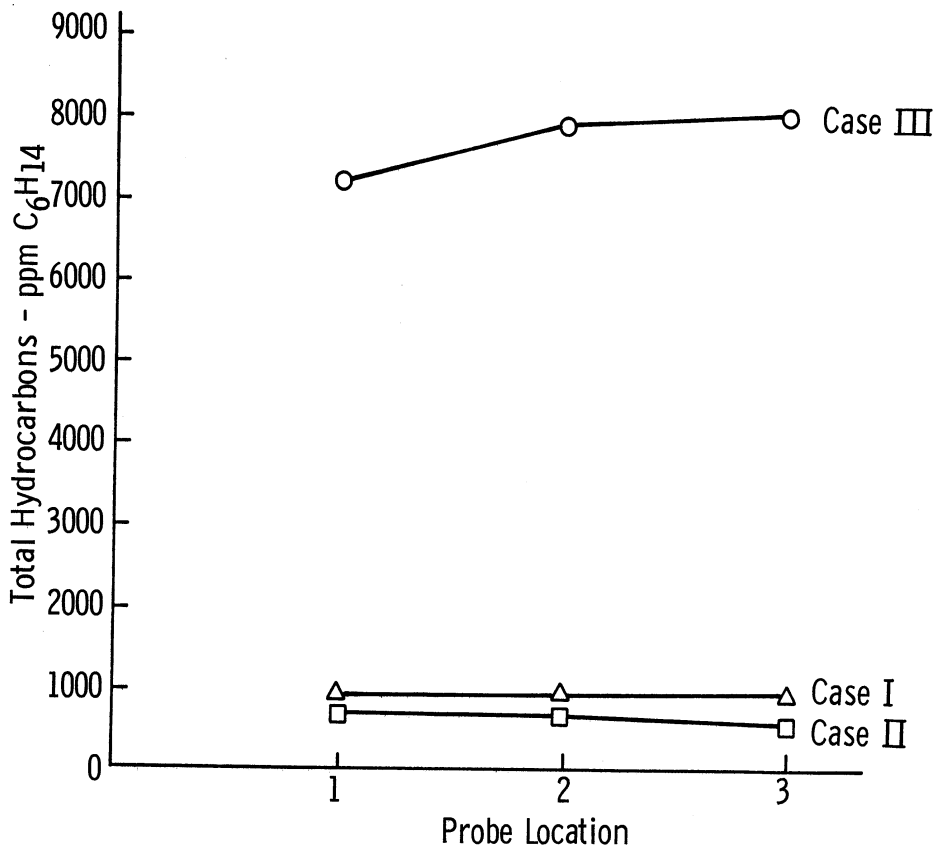

Figure 19. Total hydrocarbon concentration along the reactor flow path of the scavenging simulation.

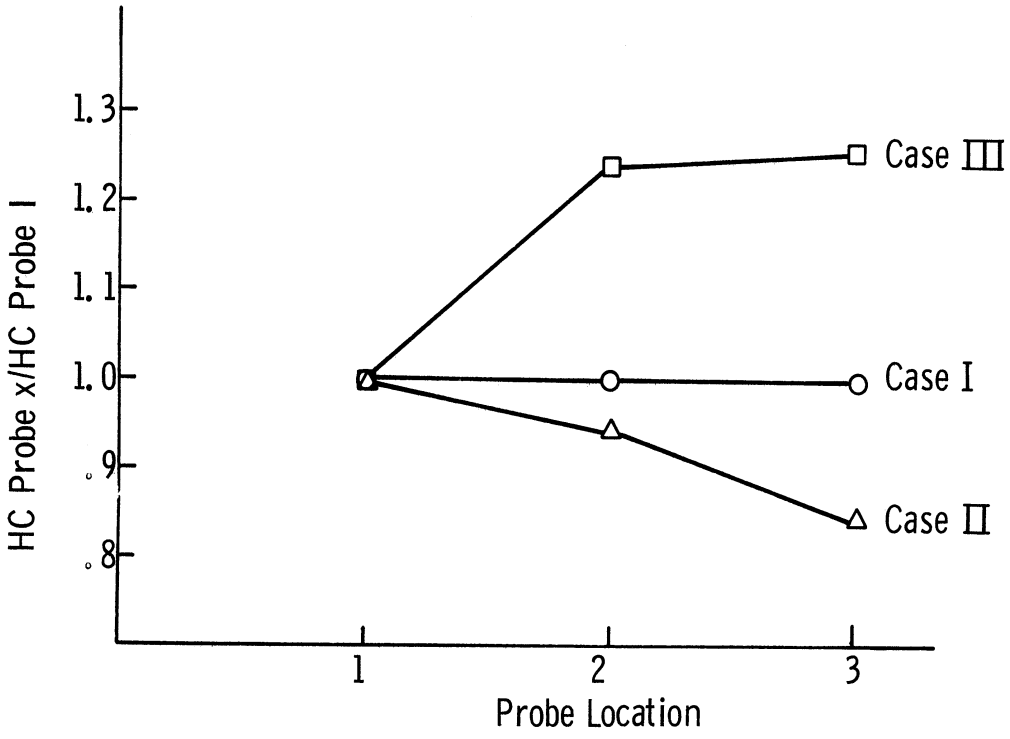

Figure 20. Hydrocarbon concentration normalized to HC data at sample probe 1, scavenging simulation.

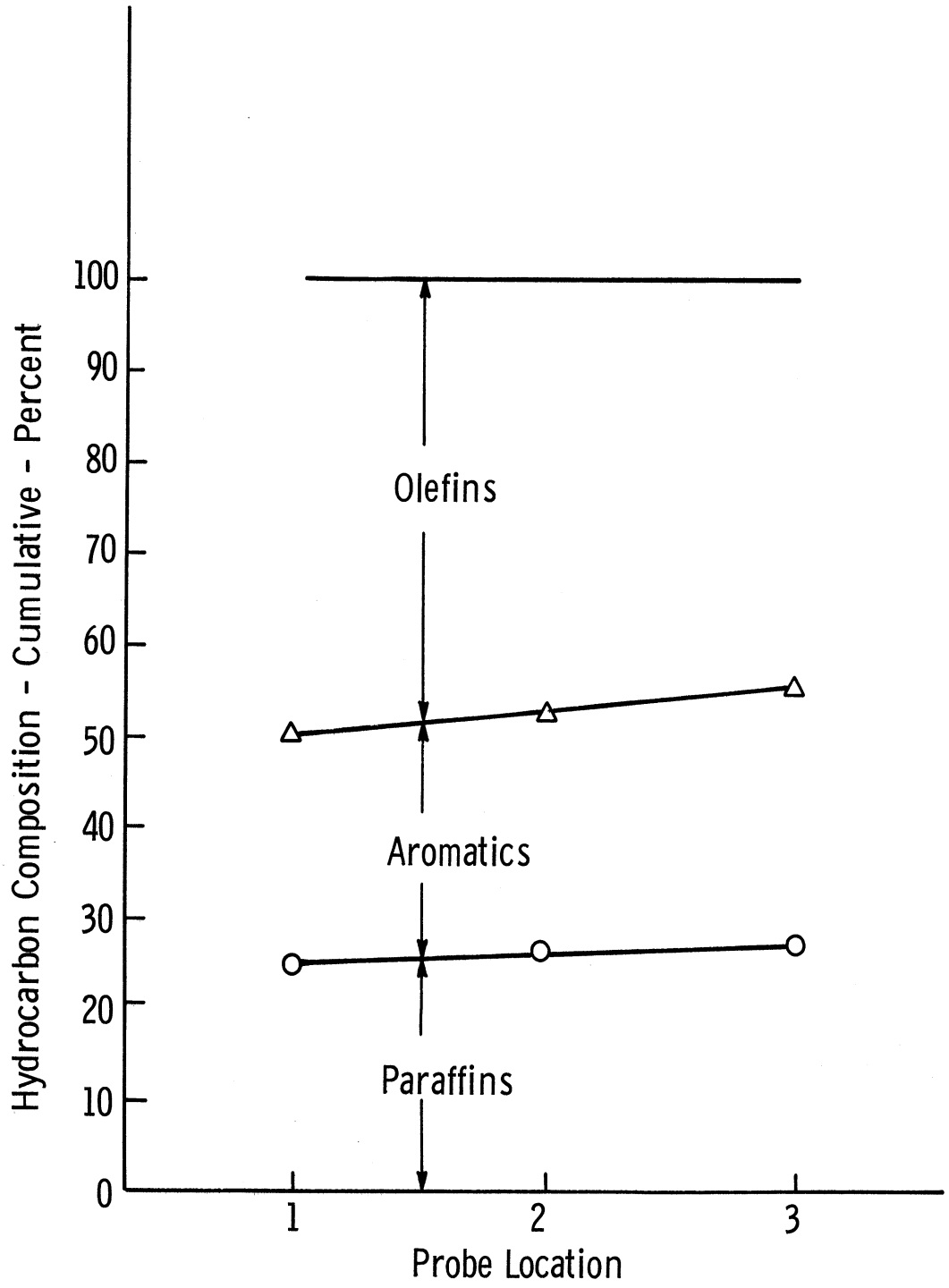

Figure 21. Family hydrocarbon composition along reactor flow path—Case I, 4-cycle exhaust only.

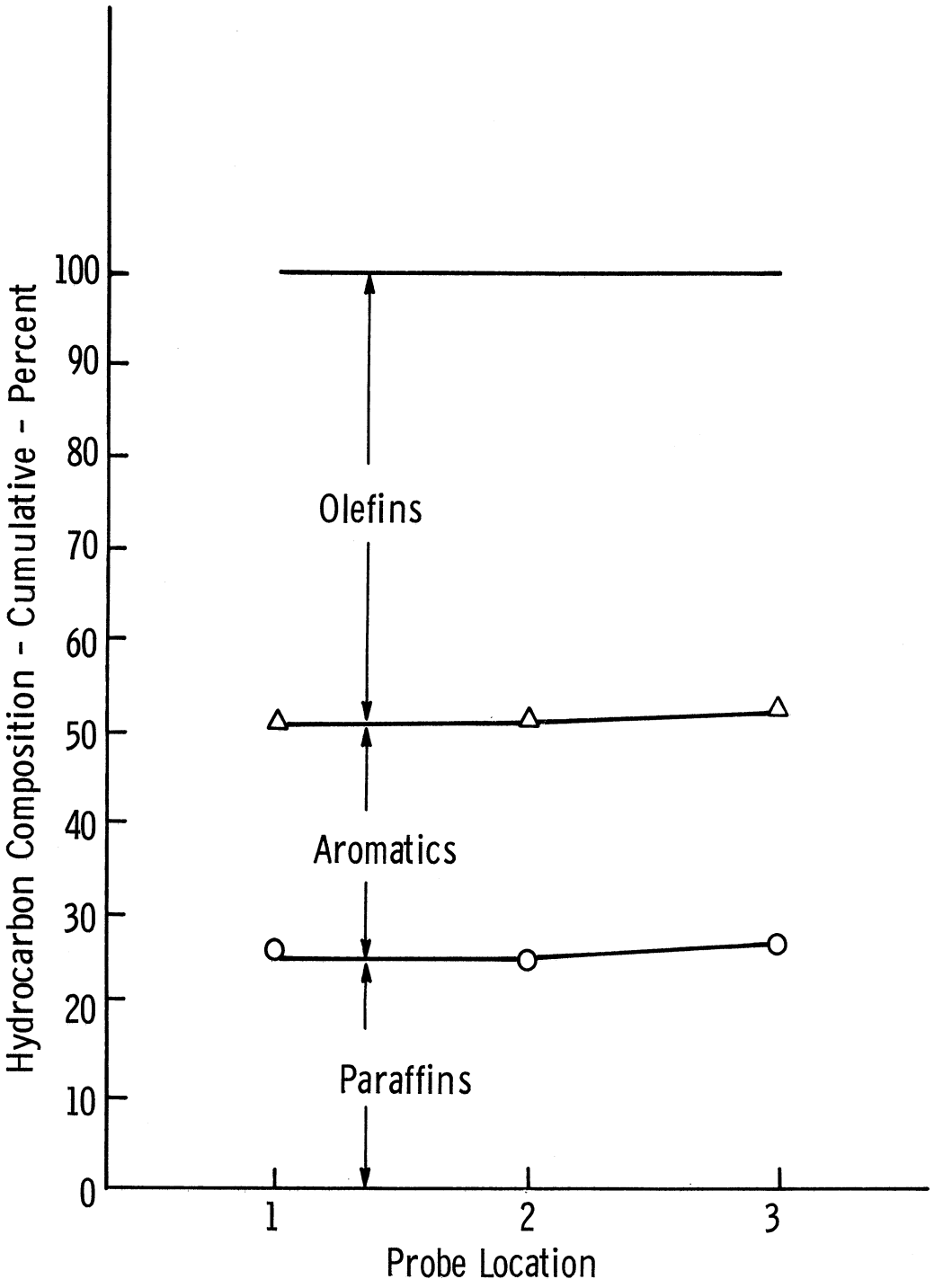

Figure 22. Family hydrocarbon composition along reactor flow path—Case II, 4-cycle exhaust plus air, $\Gamma = .75$.

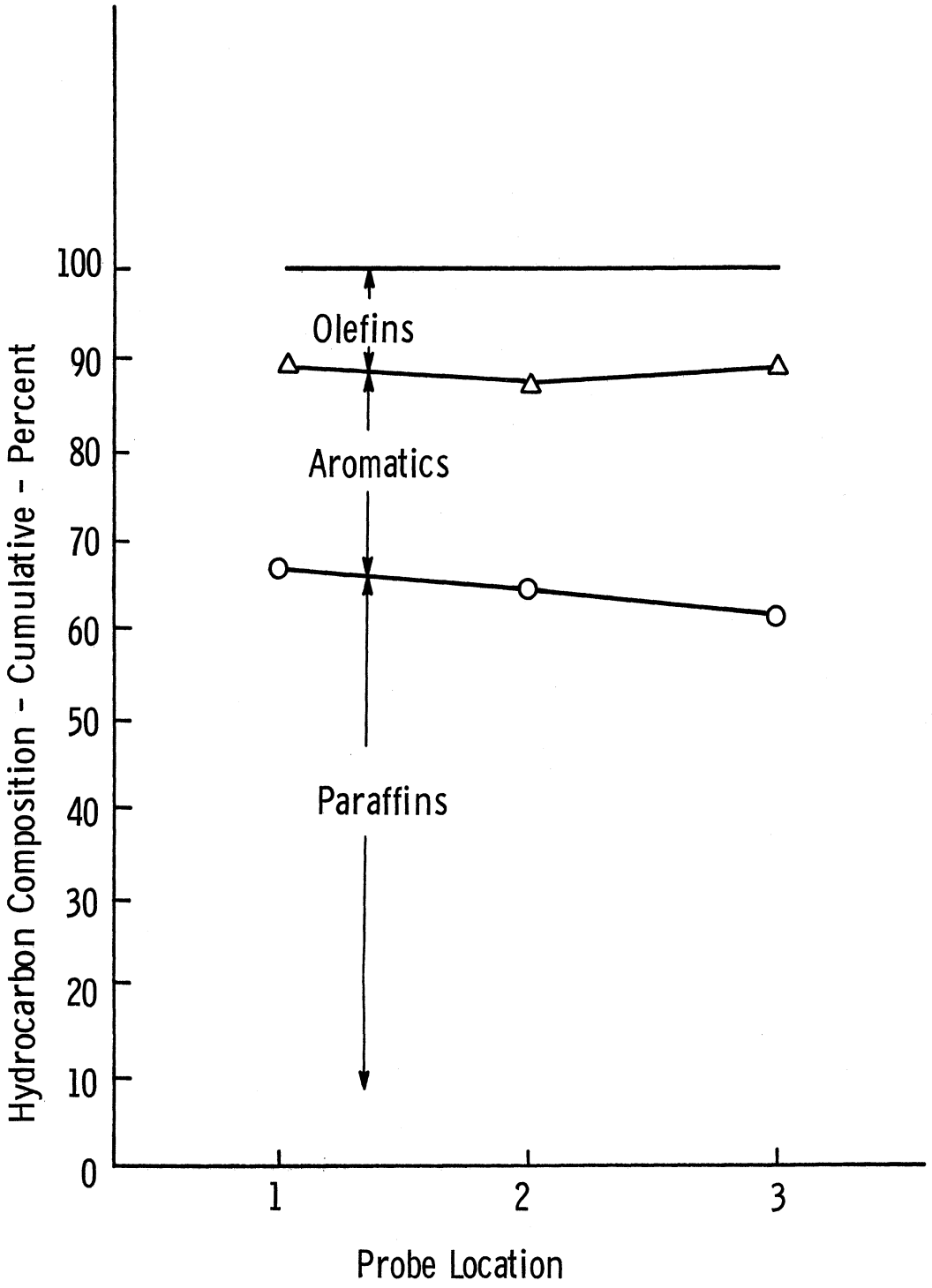

Figure 23. Family hydrocarbon composition along reactor flow path—Case III, 4-cycle exhaust plus fuel/air mixture, $\Gamma = .75$.

From the CO, CO_2, and O_2 data several observations can be made. In Case I, the CO, CO_2, and O_2 concentration is nearly constant along the reactor indicating only limited reaction. The ratio for CO/CO_2 of approximately .54 indicates the fuel/air ratio in the engine is roughly 12.7/1.

In Case II, the CO and CO_2 data is a bit erratic but there appears to be a general decrease in CO along the reactor indicating some oxidation. The O_2 concentration is, as expected, greater than Case I because of the added air and verifies the approximate setting of simulated trapping efficiency. A major fault in the experimental apparatus is indicated by the lower O_2 concentration at probe 1 which is an indication that the upstream mixer is not functioning properly. Apparently there is significant spatial composition variation across a section of the reactor. The flow along the reactor wall is probably O_2 rich and the interior flow O_2 lean in the region of sample probe 1. A study is currently being conducted to evaluate the quality of mixing by extraction of a sample from several regions of the flow cross section. This lack of homogeneity at the start of the reactor was verified in a subsequent test with the fuel/air mixture which showed a lower than expected total HC concentration at probe 1. The CO and CO_2 concentration in Case III with the addition of the fuel/air mixture suggested that the engine mixture ratio had changed from Case II to III. This was evident from a slight decrease of CO, and increase of CO_2. The O_2 results were reasonably consistent between the two runs indicating that the fraction of air added was nearly constant within expected instrumentation error.

Variability in the CO, CO_2, and O_2 concentration along the flow path causes difficulty in drawing any major conclusions, particularly in light of the expected nonhomogeneity at probe 1.

Hydrocarbon data evaluation is the major objective of this phase of the total program and does provide significant insight into the time-composition history of the unburned fuel. However, this data must be treated very qualitatively because of the poor mixing at sample probe 1.

In the test without air added, $\Gamma = 1.0$, the HC results follow the expected trend for 4-cycle engine exhaust. The total HC concentration of 900-925 ppm is consistent with similar engines operated at the same fuel/air ratio. The HC species breakdown is also consistent with other data. Of note particularly is the wide variation between fuel composition and exhaust HC composition. The paraffinic HC fraction is much lower in the exhaust (26% vs. 66%), the olefinic fraction increased very significantly (47% vs. 4%), and the aromatic content was not measurably changed. Again, this is consistent with other 4 cycle data.

Little after engine reaction was observed along the flow path in the reactor. Figure 19 illustrates this graphically. Also the family composition changes little with residence time. Certainly the lack of O_2 contributes to this behavior and is expected.

In Case II, with air only injected into the reaction chamber, the results are predictable. The total HC concentration decreased more than expected as a result of dilution of the 4-cycle exhaust and was indicative of some oxidation before probe 1. A slight decrease in HC readings was observed along the flow

path indicating that additional oxidation was occurring. These results were expected, based on experience with 4-cycle engines equipped with air injection and a thermal reactor.

The HC family composition remained nearly constant from Case I to Case II and varied little along the reactor.

Case III focused on the primary objective of the program. Both air and fuel were introduced into the hot 4-cycle engine exhaust. The total HC level increased drastically, as expected, from the other conditions. The lower total HC reading at probe 1 was probably the result of stratification across the section.

Of primary interest was the major change in HC composition with the injected fuel as shown in Figure 23. Clearly the HC composition is closely identified with the fuel. The major fraction is paraffinic, the smallest fraction olefinic, and the aromatic content is nearly constant. A detailed comparison with the composition of Indolene is not possible because the subtractive column analyzer does exhibit moderate error in family identification and the fuel composition is not exact even for Indolene. Little change in composition is observed with increasing residence time and strongly suggests that no significant oxidation of any of the HC's is occurring. Using a relatively simple calculation, the HC composition of the unreacted fuel can be determined from the subtractive column data to be:

1. Paraffins: 67%
2. Aromatics: 27%
3. Olefins: 6%

The procedure for this analysis is illustrated in Appendix B. Note that the composition indicated is well within the specification range of the fuel, Table III.

Certainly one can make a strong argument that the reactivity (based on photochemical smog formation) is less per unit of the fuel type HC than for the HC in the combustion products. Let us assign a relative reactivity number (G.M. scale) to the major HC familys as follows:

1. Paraffins: .5
2. Aromatics: 1.1
3. Olefins: 15

Admittedly these values are only approximations. It would be necessary to know the exact composition of any sample together with the reactivity of each HC species before a detailed comparison could be made. For the present analysis the raw engine exhaust is compared with the exhaust with the fuel/air mixture added, $\Gamma = .75$ simulated, collected from probe 3 in the reactor. A straight comparison on the basis of total HC yields a ratio of 9000 ppm/900 ppm = 10.

If now the proportion of the major HC families is multiplied by the appropriate relative reactivity, the photochemical smog forming potential of the two samples is in the ratio of 4.6.

The calculations are illustrated in Appendix B. From this simple calculation, it is evident that the simulated 2-cycle exhaust is a far less significant participant in the "smog" reaction than predicted by a total HC comparison. This information should have important bearing on possible future

standards for 2-cycle HC emissions. The purpose of this experiment is aimed at the goal of assessing the character of the major source of the exhaust HC, unburned fuel, as it passes through a high temperature environment. From the preliminary results, it is plainly evident that the fuel remains nearly intact, even under more extreme temperature-residence time conditions than found in the actual engine.

Testing during the final months of the test program will be aimed at verifying and amplifying the preliminary results.

B. DIRECT CYLINDER EXHAUST SAMPLING

A number of significant results were achieved with the aid of the cylinder sampling valve coupled with exhaust gas analysis. While the initial incentive was the quantitative determination of the misfiring contribution to HC emissions, several additional measurements were made including:

1. Exhaust residual dilution of the fresh charge
2. Fuel/air ratio delivered to the engine cylinder.

1. Theoretical Considerations

It is reasonable to examine the physical pre- and post-combustion processes theoretically to assist in interpreting the experimental data. The sample valve and key engine features are shown in the cylinder schematic of Figure 24. During the scavenging process, fresh mixture is attempting to both sweep the products of combustion from the cylinder and charge the cylinder. The shape of the piston head assists in deflecting the fresh mixture toward the upper portion of the cylinder to achieve thorough scavenging. However, it is

likely that the charge in the upper portion of the cylinder will consist of a greater proportion of exhaust residual than the charge in the lower section. Therefore, the measured HC concentration (at the sampling valve) should increase as the piston ascends and the charge becomes more homogeneous. With ignition and the passage of the flame past the poppet valve, the HC concentration will drop drastically although, perhaps, not to a level expected if the average HC composition of the combustion products were measured. The valve is in close proximity to the wall and lifts only several thousandths of an inch and therefore should draw an important fraction of sample from the quench layer. As the cycle progresses the flame on the average does not completely reach the extremes of the chamber. A vortex motion generated by the downward stroke of the piston may force unburned "end gas" into the center of the chamber, as shown in Figure 25. This could result in an increase in the HC concentration and should be more a pronounced factor at the low speeds and light loads (poorer combustion). Figure 26 illustrates the theoretical curve following the foregoing discussion. Also shown are theoretical curves for a total misfire and poor combustion.

2. Hydrocarbon Results

The HC data sampled from cylinder 2 is plotted in Figures 27, 28, and 29 for the 1000, 2000, and 3000 rpm test conditions. For reference the ignition crank angle and the average crank angle at which the flame arrived at the

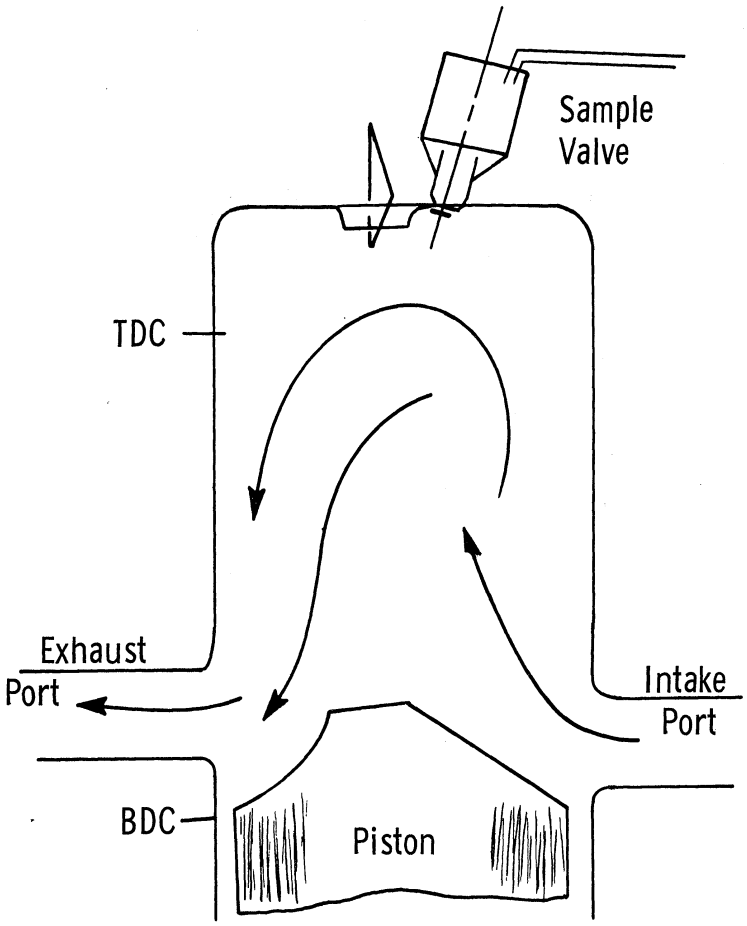

Figure 24. Schematic diagram of cylinder 2 of the Johnson test engine with the Cox valve installed.

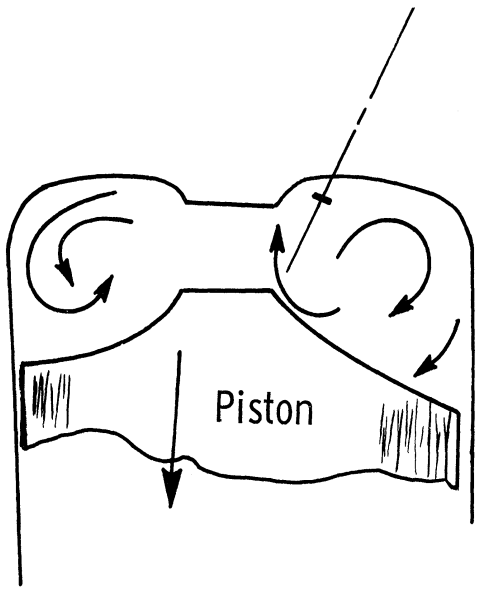

Figure 25. Hypothesized gas motion in engine cylinder during the expansion stroke.

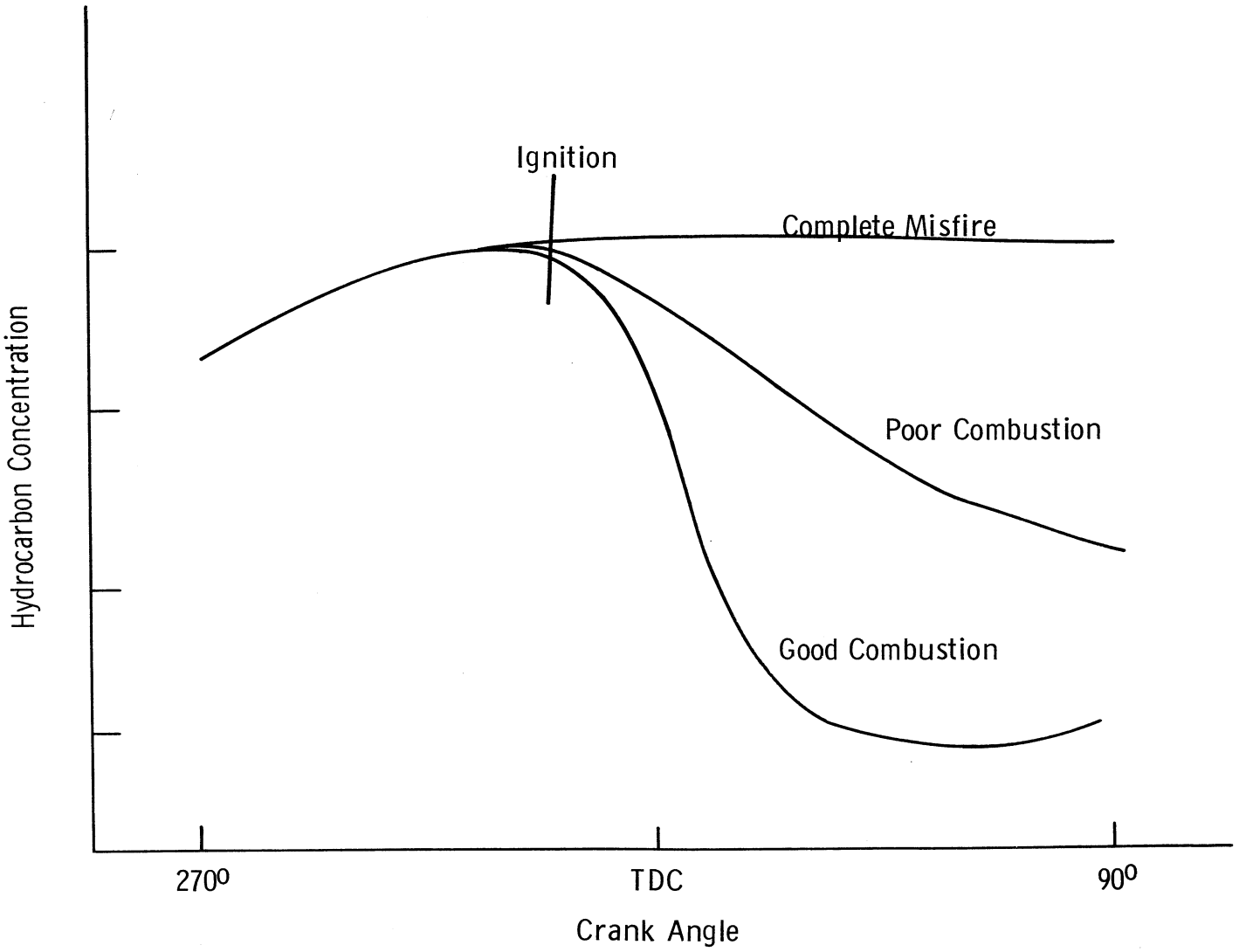

Figure 26. Theoretical curves of hydrocarbon concentration as a function of crank angle.

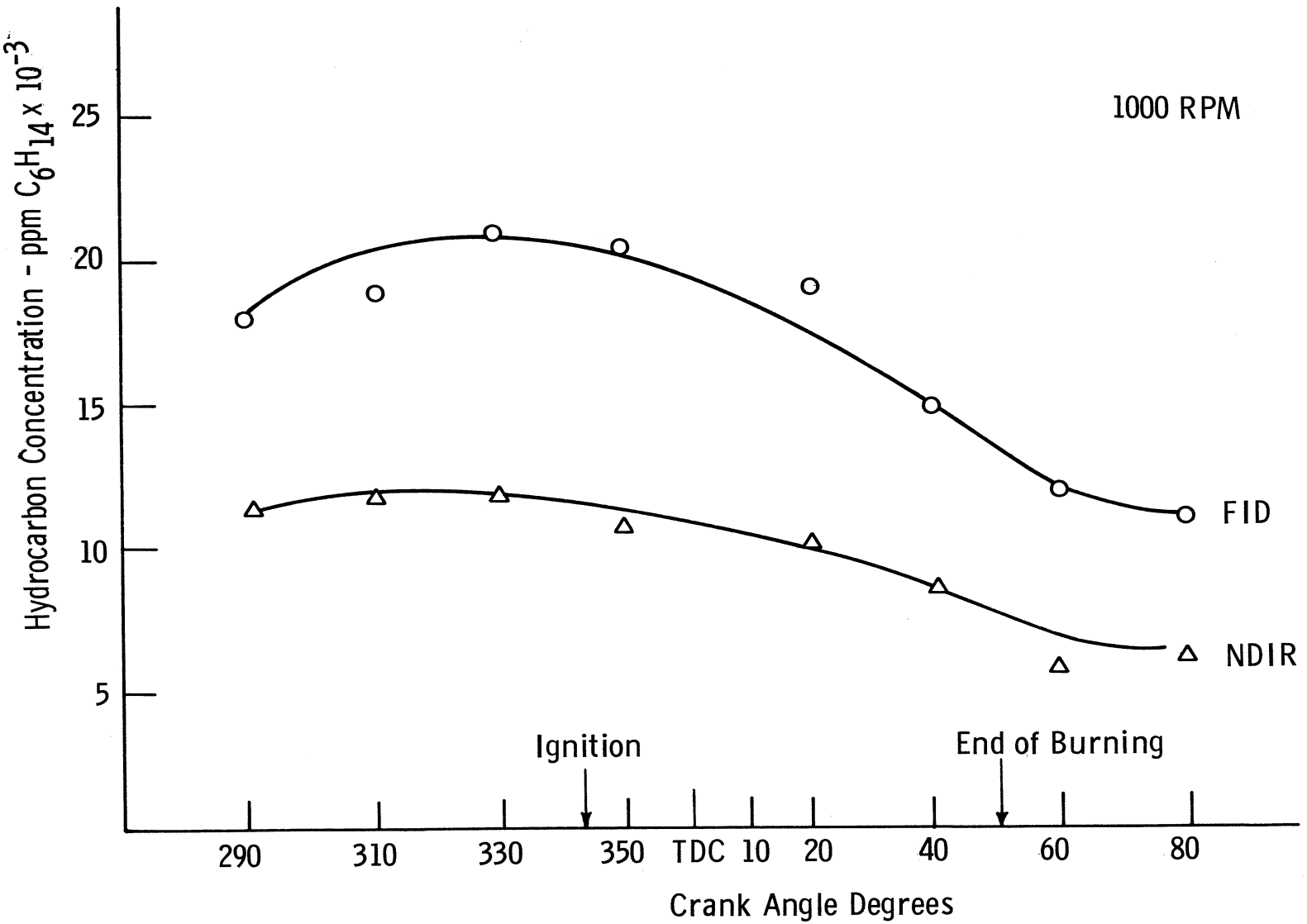

Figure 27. Hydrocarbon concentration, FID and NDIR, as a function of crank angle in cylinder 2—1000 rpm, boat load.

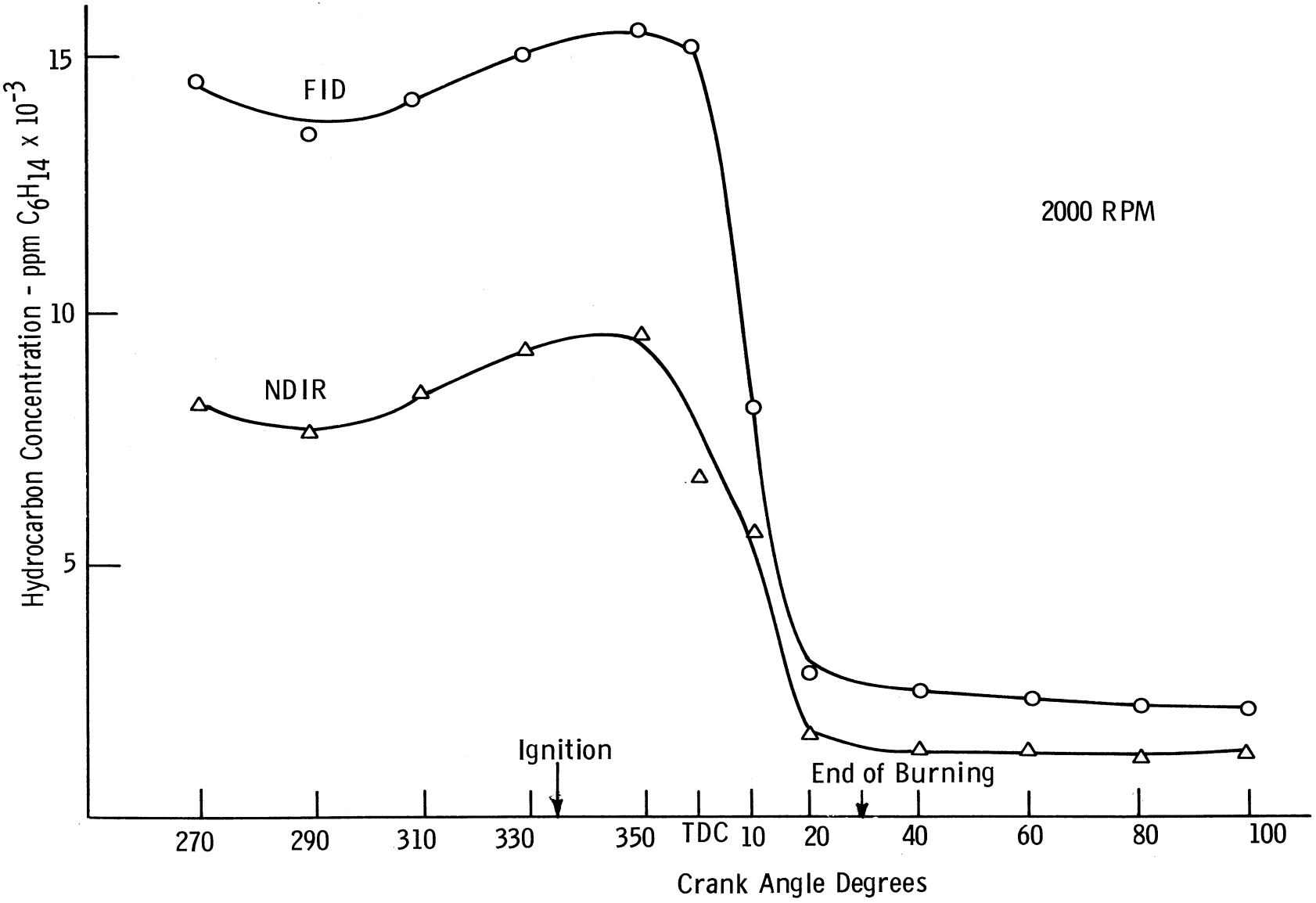

Figure 28. Hydrocarbon concentration, FID and NDIR as a function of crank angle in cylinder 2—2000 rpm, boat load.

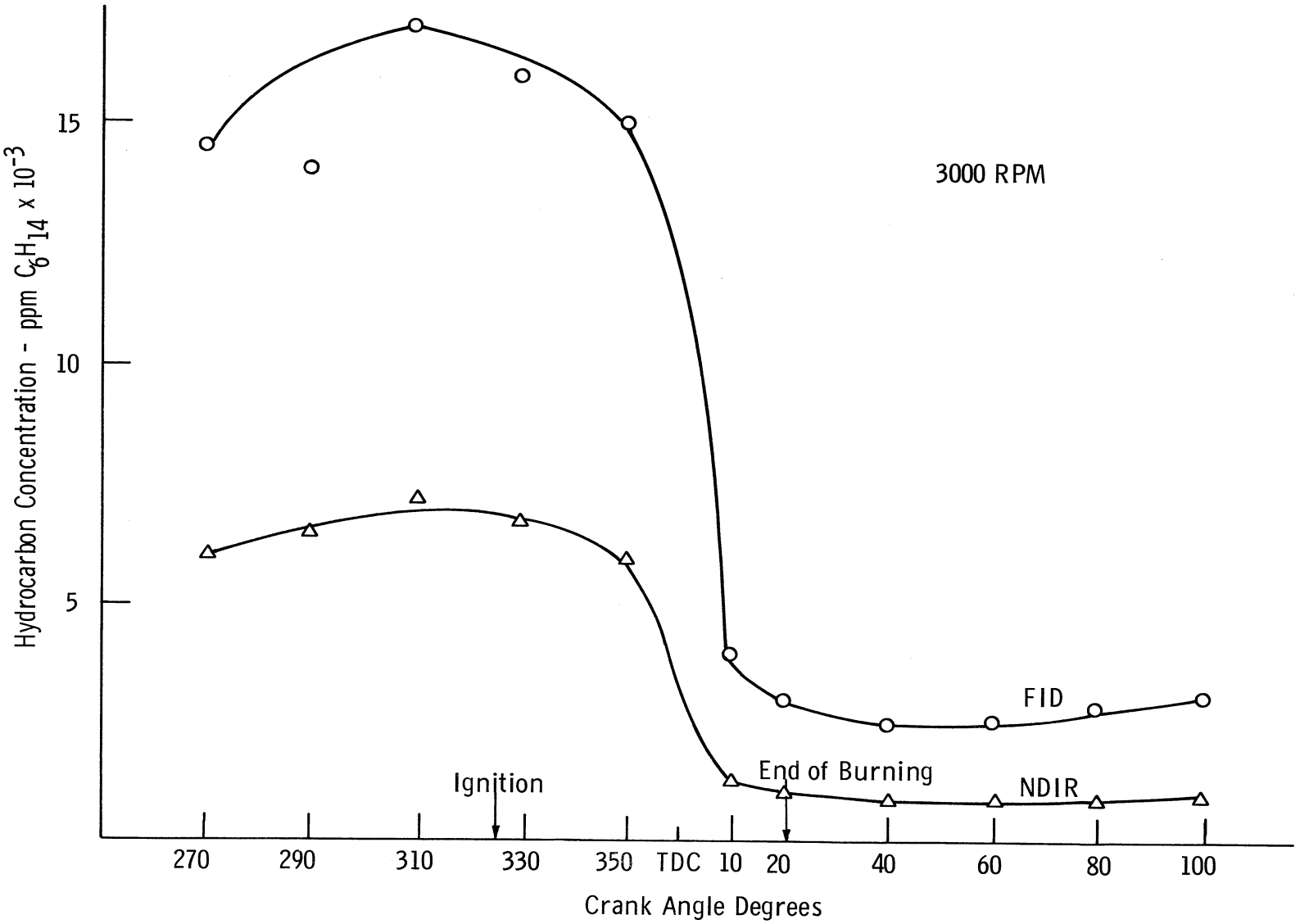

Figure 29. Hydrocarbon concentration, FID and NDIR, as a function of crank angle in cylinder 2—3000 rpm, boat load.

farthest extremity of the chamber.* A complete summary of all emission average data including the HC concentrations is shown in Tables V, VI, and VII.

It must be observed that the plotted crank angle represents the angle of valve opening and not the midpoint angle of valve opening. The valve is open (dwell angle) for several milliseconds which represents several crank degrees and this dwell angle increases with engine speed. The sample obtained is the average over several degrees of crank angle.

As indicated in the theoretical discussion, HC concentration rises slightly just before combustion and then decreases rapidly as the flame passes the sample valve. Generally there was no increase in the HC composition near the end of the power stroke as suggested from theoretical considerations. However, a slight upturn was observed with the NDIR results at 1000 rpm and FID data at 3000 rpm.

At 1000 rpm the HC decrease was small with flame passage because of incomplete combustion due to excessive residual dilution. Both the NDIR and FID results at the end of expansion were approximately 35% greater than the exhaust port HC data. This discrepancy was probably due to a combination of "crosstalk" from other cylinders in the exhaust port, imperfect sampling, and the fact that the combustion was not complete at the last crank angle of sampling. The gradual decrease of HC concentration with expansion is probably due to a relatively slow HC oxidation, but the evidence from this run is not

*The crank angle at which the flame arrived at the extremity of the chamber was determined with an ionization probe located at this position. The flame speed varies from cycle to cycle and therefore this crank angle is the average for many cycles.

TABLE V

EMISSION AT 1000 RPM AS A FUNCTION OF CRANK ANGLE DATA

Crank Angle	HC-NDIR ppm	HC-FID ppm	FID/NDIR	O_2 (%)	CO_2 (%)	CO (%)	CO_2/CO	A/F
290	11200	18000	1.61	15.5	2.0	2.7	.740	10/1
310	11600	19000	1.64	15.7	2.0	2.7	.740	10/1
330	11600	21000	1.82	15.5	2.0	2.7	.740	10/1
350	10600	20500	1.96	13.5	3.1	3.7	.888	10.5/1
20	10000	19000	1.90	14.5	2.5	3.3	.757	10/1
40	8400	15000	1.78	8.3	4.9	6.3	.778	10/1
60	5900	12000	2.03	5.0	6.8	8.1	.846	10.5/1

TABLE VI

EMISSION AT 2000 RPM AS A FUNCTION OF CRANK ANGLE DATA

Crank Angle	HC-NDIR ppm	HC-FID ppm	FID/NDIR	O_2 (%)	CO_2 (%)	CO (%)	CO_2/CO	A/F
270	8100	14500	1.79	16.8	2.6	2.3	1.13	11/1
290	7600	13500	1.78	15.5	2.4	2.0	1.20	11/1
310	8400	14200	1.69	15.2	2.3	2.2	1.04	11/1
330	9100	15000	1.67	15.4	2.5	2.4	1.04	11/1
350	9450	15500	1.64	14.7	2.8	2.6	1.08	11/1
0	6700	15200	2.27	9.5	4.8	2.6	1.09	11/1
10	5500	8000	1.45	5.6	6.2	6.0	1.03	11/1
20	1500	2800	1.87	.5	9.0	7.8	1.15	11/1
40	1400	2500	1.78	.7	9.0	7.2	1.25	11.5/1
60	1300	2300	1.77	.8	9.2	7.2	1.28	11.5/1
80	1200	2100	1.75	.3	9.2	7.4	1.24	11.5/1
100	1200	2100	1.75	.5	9.2	7.2	1.28	11.5/1

TABLE VII

EMISSION AT 3000 RPM AS A FUNCTION OF CRANK ANGLE DATA

Crank Angle	HC-NDIR ppm	HC-FID ppm	FID/NDIR	O_2 (%)	CO_2 (%)	CO (%)	CO_2/CO	A/F
270	6000	14500	2.42	15.9	2.8	.7	4.00	13.5/1
290	6400	14000	2.19	16.5	2.5	.6	4.16	13.5/1
310	7100	17000	2.39	16.4	2.4	.7	3.43	13.0/1
330	6700	16000	2.39	15.0	3.5	1.2	2.91	12.8/1
350	5900	15000	2.54	2.7	10.0	4.4	2.27	12.0/1
10	1350	4000	2.96	0.0	12.0	5.8	2.07	12.0/1
20	1000	3000	3.00	0.0	14.0	4.0	3.50	13.0/1
40	800	2500	3.12	0.0	13.5	5.0	2.70	12.6/1
60	800	2500	3.12	.1	13.0	5.4	2.41	12.0/1
80	850	2800	3.30	.5	12.5	5.1	2.45	12.5/1
100	1000	3000	3.00	.4	12.5	4.9	2.55	12.5/1

conclusive because the sample is obtained at only one location at each instant in time. However, it is believed that the valve does draw a reasonably representative sample considered over a large crank angle. With each angle the valve draws a sample from a new section of the gases (new gases are swept into the sampling region). The gases should be increasingly homogenized with time, including the "quench" region in the vicinity of the sample valve.

Hydrocarbon concentration at higher speed runs remains almost constant with crank angle after combustion and strongly suggests that the sample obtained at any crank angle is representative of the bulk gases. This tends to support the conclusion that the 1000 rpm post-combustion results is a true measure of the bulk gas HC composition and, in fact, the HC decrease with crank angle is due to after-reaction. The pre-combustion FID measurement was somewhat higher than expected with the unheated FID analyser and was very close to the total HC value predicted from the fuel/air ratio.

The HC data at 2000 and 3000 rpm are very similar. Clearly, the burning is far more complete than at 1000 rpm. A slight anomaly was observed between the data. The pre-combustion NDIR results were higher at 2000 rpm that at 3000 rpm, but the FID data was in the reverse order. No explanation is apparent for this occurence but generally the FID results at 3000 rpm were more erratic.

3. CO, CO_2, and O_2 Test Results

The CO, CO_2, and O_2 data are presented in Tables V, VI, and VII and are plotted as a function of the valve opening crank angle in Figures 30, 31, and 32 at the three test conditions.

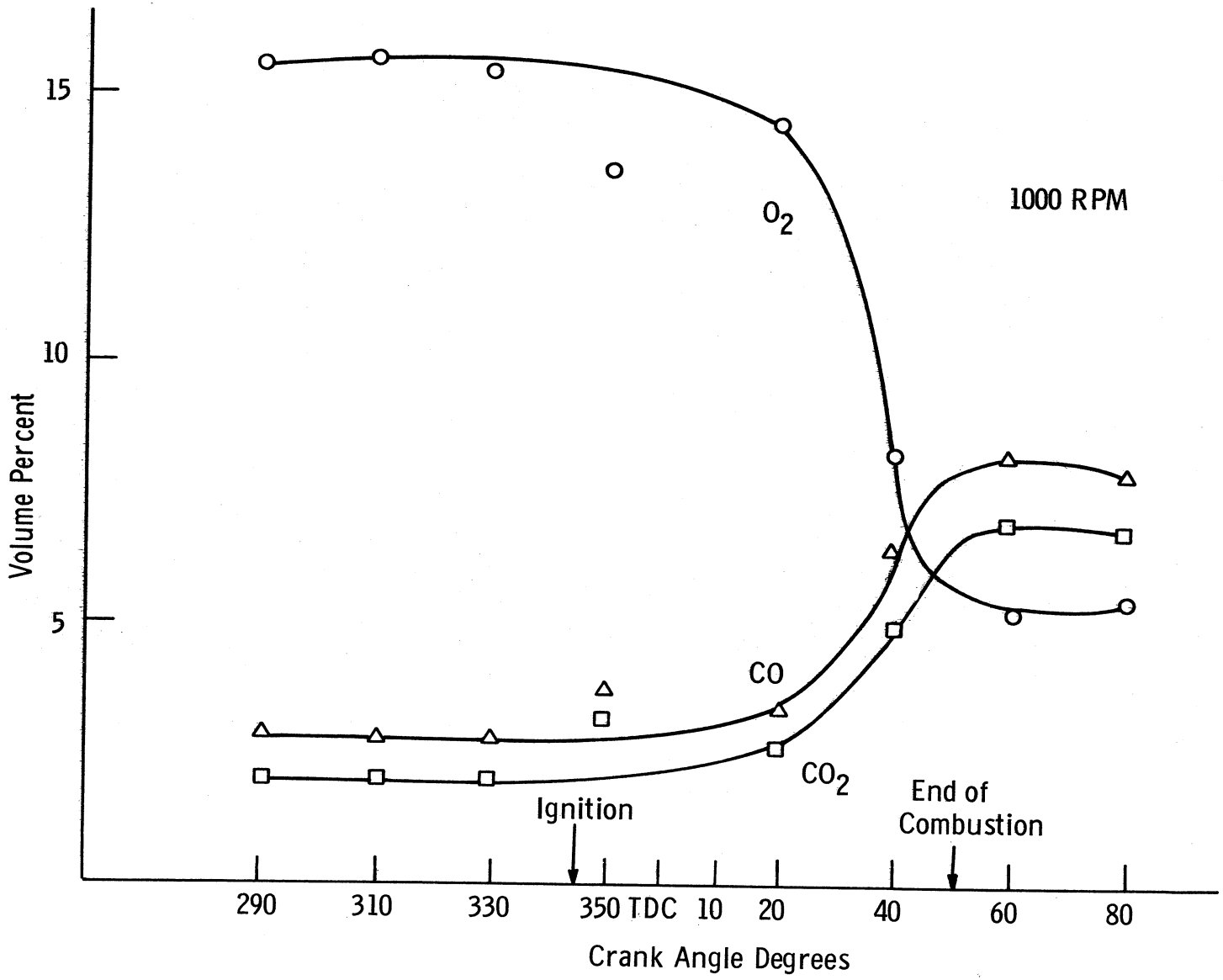

Figure 30. Carbon monoxide, carbon dioxide, and oxygen concentration as a function of crank angle in cylinder 2—1000 rpm, boat load.

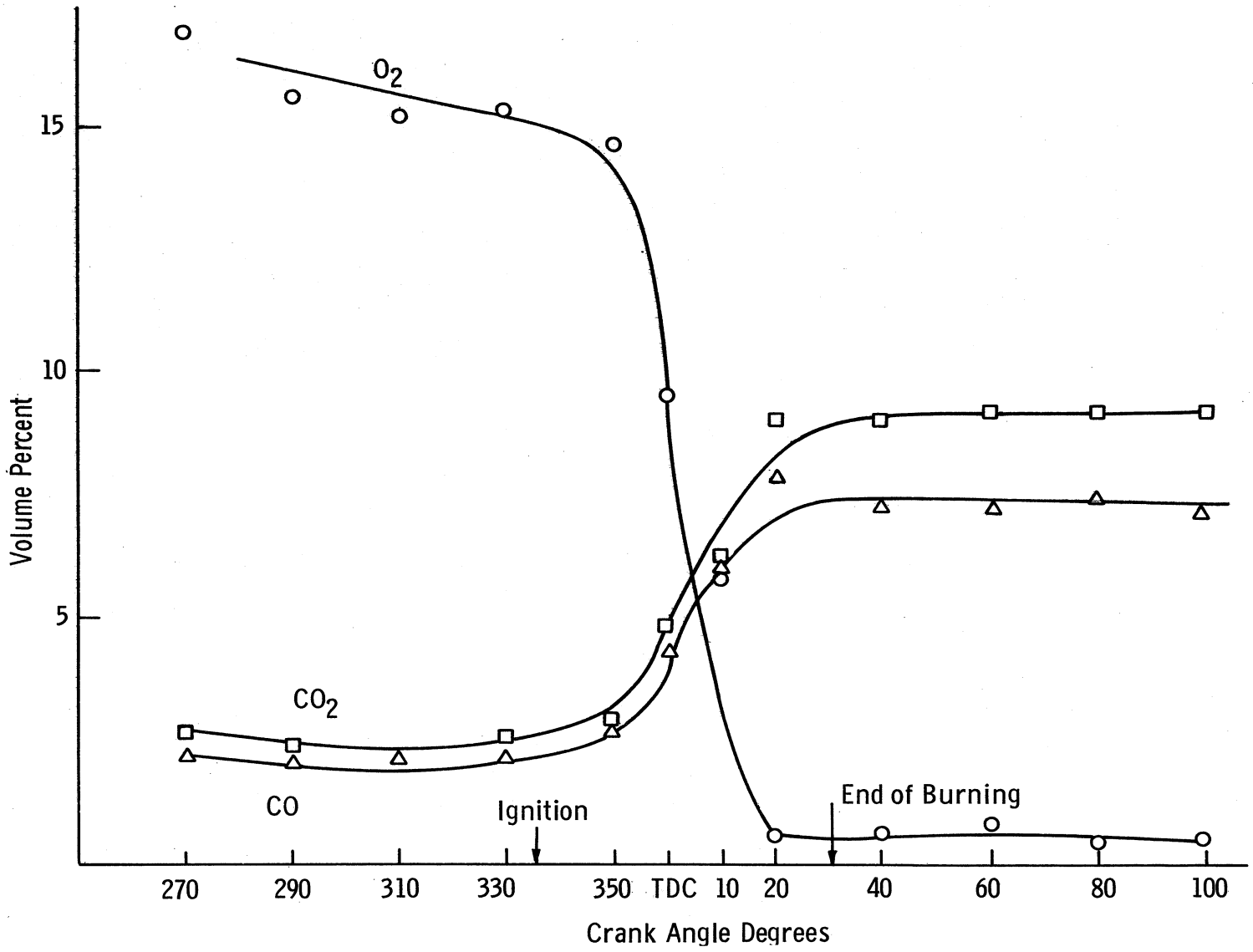

Figure 31. Carbon monoxide, carbon dioxide, and oxygen concentration as a function of crank angle in cylinder 2—2000 rpm, boat load.

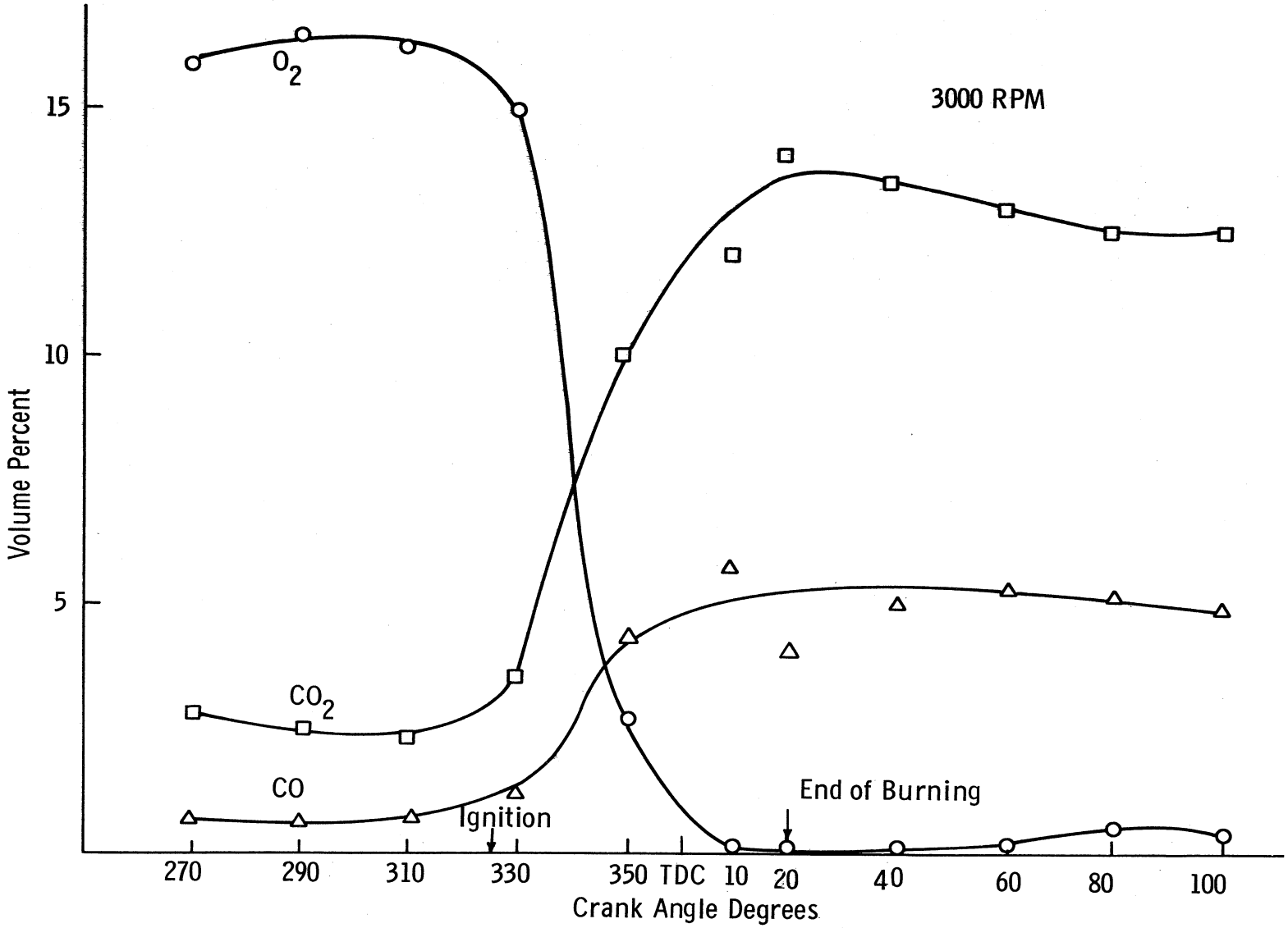

Figure 32. Carbon monoxide, carbon dioxide, and oxygen concentration as a function of crank angle in cylinder 2—3000 rpm, boat load.

Clearly the transition from pre-combustion through combustion, to post-combustion is again evident at all test conditions. The ratio between the CO/CO_2 remains essentially constant throughout the test at each speed, as does the individual concentrations during both the pre- and post-combustion sampling.

The consistent individual readings again suggest that the gas is relatively homogeneous and the sample withdrawn is reasonably representative of the bulk gases at any instant. Furthermore, the nearly constant CO/CO_2 ratio means that the measured fuel/air is constant (within limits of instrumentation error) as a function of crank angle which, in fact, must be true. Significant variation in this ratio would have raised serious doubts as to the validity of the data. Fuel/air ratio observations will be discussed in a subsequent section.

The O_2 results were, as expected, essentially the inverse of the CO and CO_2 results.

4. FID/NDIR Hydrocarbon Ratio

From past experience it was believed that the ratio of the FID to NDIR hydrocarbon data would be useful in assessing the basic nature of the HC composition. As discussed in a previous report the NDIR analyzer is primarily sensitive to paraffinic HC's, whereas the FID effectively measures the total, nonoxygenated HC content of the sample. Since the fuel is highly paraffinic and the HC content of the quench zone exhibits a much smaller fraction of paraffins, the FID/NDIR ratio is a qualitative measure of the source of the HC in the sample.

A large ratio suggests a small fraction of fuel is present and small ratio suggests that the HC are not closely related to the fuel. In the exhaust emission studies of the previous year, the FID/NDIR ratio was consistently in region of 1.3-1.5. These results strongly supported our hypothesis that two cycle exhaust HC content is primarily due to overscavenging and misfiring. The results of the present effort were shown in Tables V, VI, and VII and are plotted in Figure 33.

Clearly one would expect the pre-combustion charge to yield a lower FID/NDIR ratio than the products and this was in evidence for all tests, but the change was much smaller than expected. The 1000 and 2000 rpm pre-combustion results were higher than the previous exhaust emission studies revealed (average of 1.7 vs. 1.3). The 3000 rpm data was significantly different (2.3 vs. 1.3). No explanation is readily obvious for this discrepancy and, in fact, it was expected that the ratio would be less than 1.5. One possible explanation may be related to the temperature of the gases during pre-combustion sampling. They were certainly at a substantially lower temperature (because of the cooling effect of the mixture) than the exhaust gases. This may have caused "hang up" of the heavier HC's in the sample system and if these were highly paraffinic the FID/NDIR ratio could be increased. No species breakdown of the fuel is available to facilitate validation of this theory. Also there is some reason to question the performance of the FID at the very low sample flow rates used in this study. The unit was operated near its "limit of performance" and major errors are entirely possible. Another factor which may be of importance relates to O_2 interference. No attempt was made to

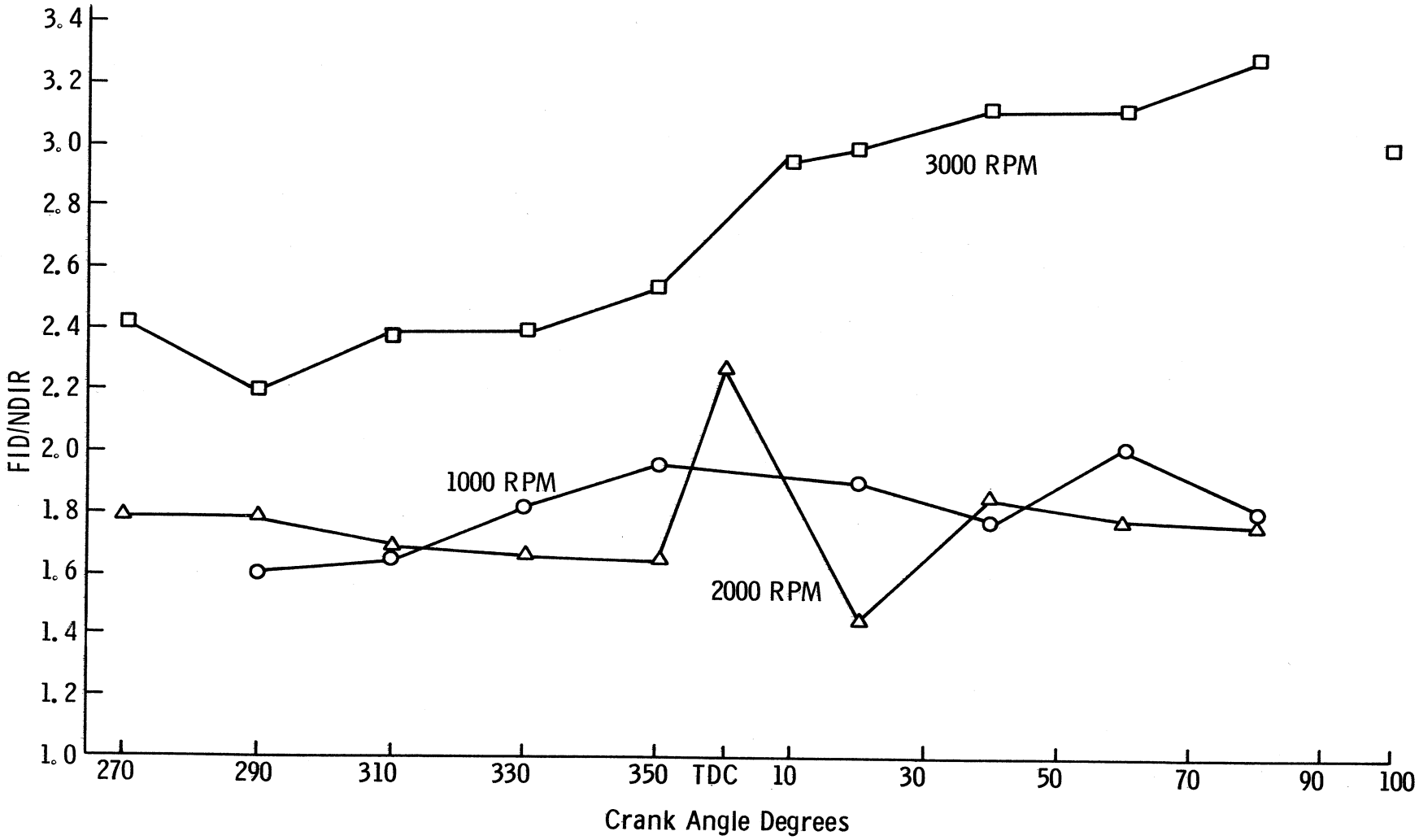

Figure 33. Ratio of FID/NDIR hydrocarbon concentration as a function of crank angle—1000, 2000, and 3000 rpm, boat load.

correct the data because reliable correction curves were not available at the FID instrument settings used. The settings were substantially different from those used in previous exhaust analysis work where O_2 interference was carefully checked. Reference gases with known O_2 concentrations are no longer available.

5. Misfiring Analysis—Direct Cylinder Sample

The misfiring frequency or fraction of the trapped charge that burns can be readily computed from the pre- and post-combustion data. The mathematical relationships are developed and explained in Appendix D for both misfiring and exhaust residual dilution of the charge. Actually, it initially appeared that three constituents; CO, CO_2, and O_2 could be used for this calculation and provide a valuable cross check. However, substantial error could be introduced in the computations if even a small error was made in the fuel/air ratio, note Appendix D. Calculations using the CO_2 and CO results require a precise knowledge of the chemical reaction equation coefficients for CO_2 and CO in the complete products. An error of half an A/F ratio can result in more than a 20% error in the misfiring measurement or the average "completeness" of combustion. For this reason, only the results from the O_2 analysis are reported. Figure 34 shows the average fraction of trapped charge that is burned at the 1000, 2000, and 3000 rpm test conditions. In this test the only appreciable incomplete burning occurred at 1000 rpm. This data certainly verified the trends observed with the ionization probe results, but placed a quantitative value on the "completeness" of combustion. Actually, it was

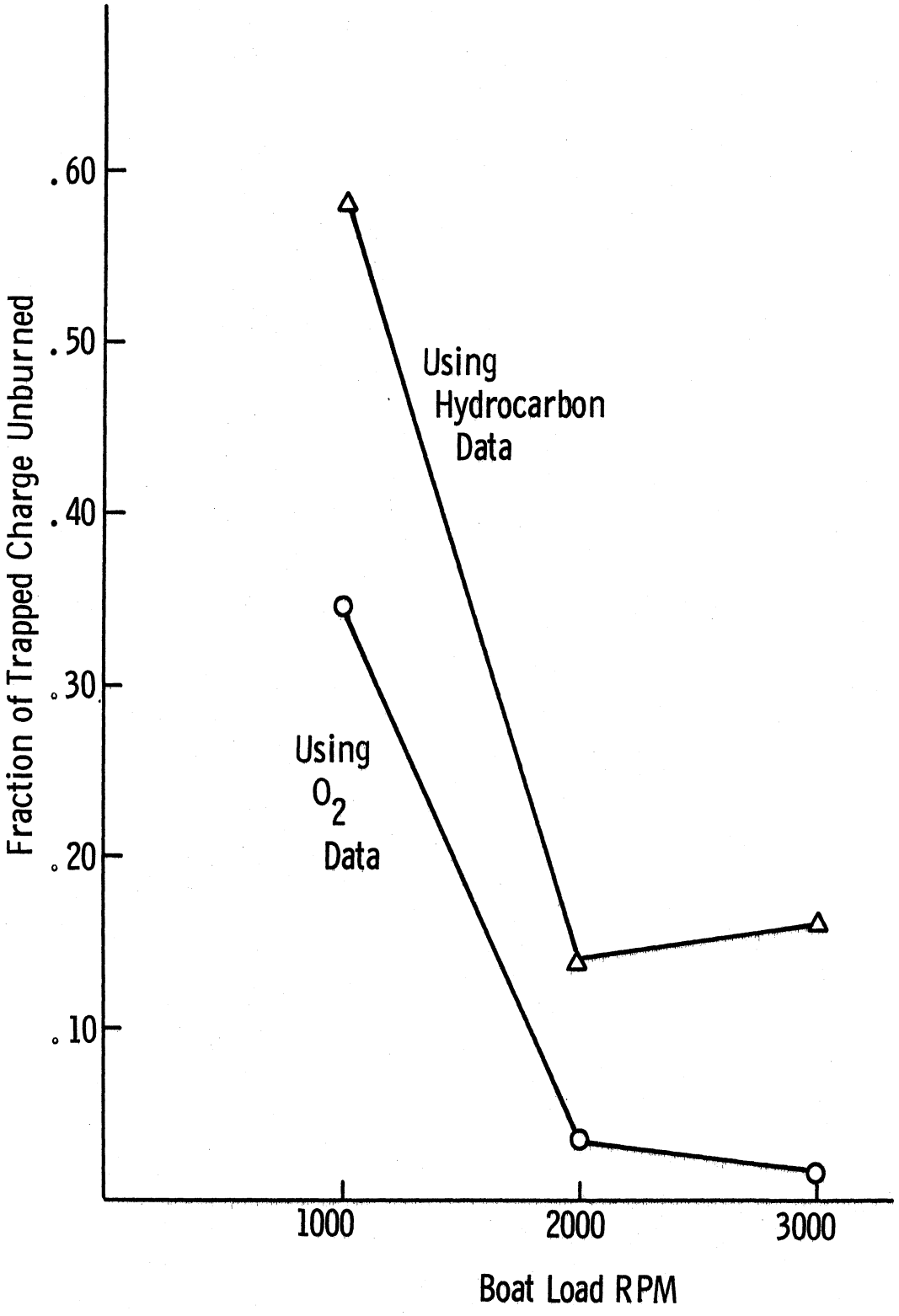

Figure 34. Fraction of trapped charge unburned in cylinder 2 at 1000, 2000, and 3000 rpm, boat load.

surprising to see efficient burning at 2000 and 3000 rpm in light of the significant residual dilution of the charge at these conditions. This will be discussed in the following section.

The pre- and post-combustion HC data (FID) were also considered for use in this analysis. Only the FID data was used because of the expected major change in HC family composition with combustion. The NDIR analyzer responds nonlinearly to the various HC families. The results are also plotted in Figure 32. The completeness of burning indicated was significantly less than for the O_2 technique. The discrepancy is likely related to a combination of several factors:

1. The post combustion HC data is probably high because the sample may contain a slightly greater proportion of the quench zone gases which are HC rich. The 1000 rpm data is particularly suspect because of the very slow burning.

2. The O_2 analyzer generally exhibits less accuracy than the other emission analyzers used, although any error would probably cause the O_2 results to be higher than the actual.

3. It was assumed that HC and O_2 fraction in the complete products of combustion were zero. This is a most risky assumption with the rich and probably nonhomogeneous mixtures used.

In any event, the data does appear to provide significant insight into the problem of incomplete burning. The O_2 data is believed to be the most accurate. However, substantial additional testing would be necessary to verify this conclusion.

6. Residual Dilution of the Charge

The two-cycle engine is generally considered to have a significant problem with exhaust residual dilution of the fresh charge. This is

particularly true at the low speed and load conditions where scavenging is relatively inefficient. Very rich mixture ratios are required to attain the best power condition. With the sample valve and exhaust analysis it is possible to quantify the degree of residual dilution. The calculation procedure is indicated in Appendix D using three different exhaust constituents, CO_2, CO, and O_2.

Sample results are plotted in Figure 35 and show the residual fraction in the charge as a function of the test condition. At each condition the residual fractions calculated from the three constituents are within 5% of each other, certainly strengthening the validity of the results.

At the 1000 rpm condition the residual dilution is substantial, 32%. Even at the 2000 and 3000 rpm test points the dilution is significant and explains the very low NO emission readings of an earlier study. In effect the 2-cycle engine possesses significant internal exhaust gas recirculation (EGR). Residual dilution of this magnitude markedly reduces the thermodynamic efficiency of the cycle and, in addition to overscavenging and nonoptimum spark advance, readily explains the high BSFC at low speed and load. This technique appears to possess merit as a tool for the assessment of 2-cycle scavenging efficiency.

The results suggest that the scavenging efficiency of cylinder 2 of the test engine is relatively poor.

C. ION PROBE MISFIRING ANALYSIS

Limited effort was put into the ionization probe misfiring analysis because it was viewed to be of less value than the other segments of the

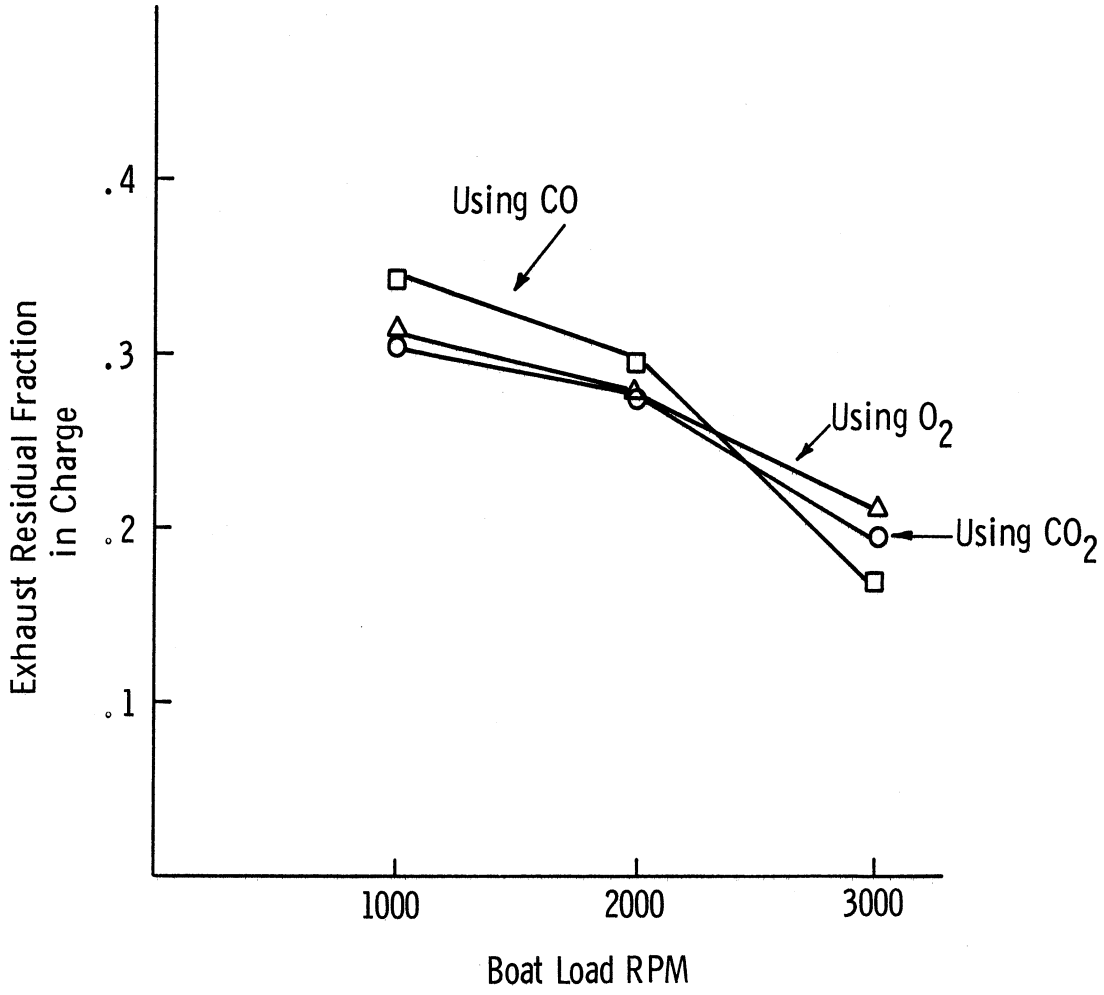

Figure 35. Exhaust residual dilution of fresh charge in cylinder 2 at 1000, 2000, and 3000 rpm, boat load.

program. Results were obtained which clearly show misfiring or poor combustion to be an important source of HC emissions at the low speed and load test conditions. Therefore, testing was concentrated in this region. Qualitatively the data agreed favorably with the cylinder gas sampling technique.

With the multiple (3) ion probe system in cylinder 2, the frequency of flame passage past the ion gaps was determined over a large number of cycles. Unfortunately, the electronics did not permit a sequential analysis over each cycle. Rather, the arrival or nonarrival of the flame at a given probe was determined over a large number of cycles. Then the next ion probe was checked over many cycles. This was believed to be a reasonable practice because the engine operation appeared to vary little in the relatively short periods involved.

It was found that the voltage generated in the external circuit varied considerably. The maximum voltage pulse was electronically adjusted to 10 V. Varying voltage pulses of from 0 to + 10 V were generated. It was decided arbitrarily to consider a voltage pulse of 2 V or less as "no combustion" at the ion gap. The count was controlled electronically such that a trigger pulse was generated by another electronic system with a 2 V or greater input signal from the ion-probe.

An example of the new data and triggering pulses for the three ion probes is shown in Figure 36. Probe 1 was located very close to the ignition source, probe 2 approximately at half the chamber radius, and probe 3 at the extreme of the chamber. The count pulse is shown at the top of each photograph and the ion-gap voltage in the lower part. Note that the flame passes probe 1

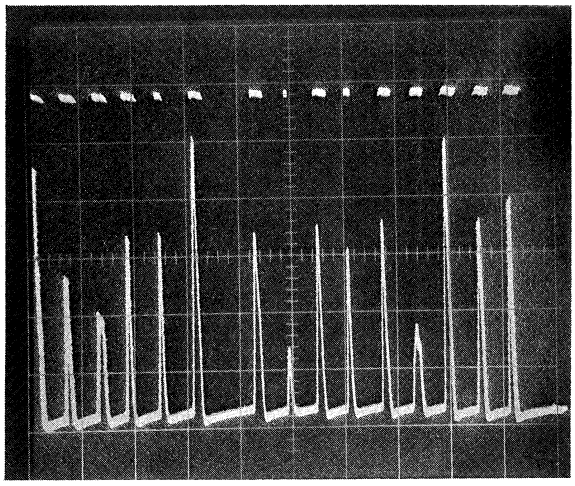

ION-PROBE

No. 1 (closest to ignition source)

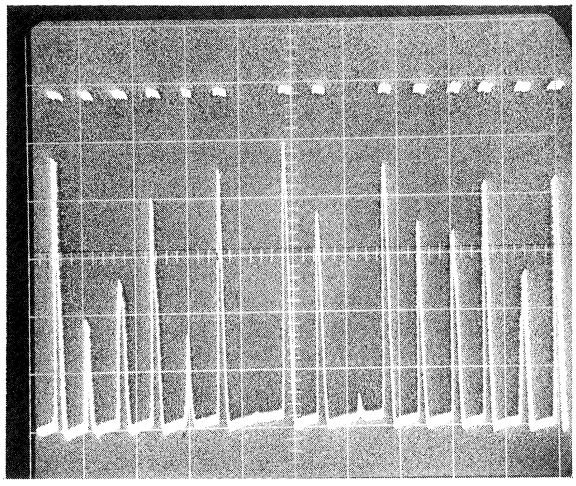

No. 2

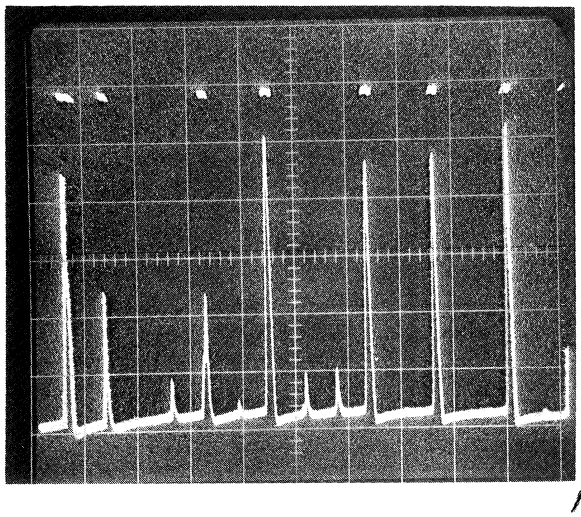

No. 3

1000 rpm, boat load

Figure 36. Sample ionization probe misfiring data from cylinder 2 at 1000 rpm, boat load.

much more frequently than it arrives at probe 3 and indicates that burning is often quite incomplete.

A sample data set is shown in Appendix E. The results proved to be surprisingly reproducible after several electronic problems were solved. Perhaps the most significant problem resulted from a multiple voltage pulse which randomly occurred with the passage of the flame past the probe. This is illustrated in Figure 37. Two count pulses could be generated by a single flame passage. This problem was alleviated by using a "Schmitt trigger" arrangement which sensed the first voltage rise and rejected any additional pulses on a given cycle.

A large quantity of data was averaged and is summarized in Figure 38. Three test conditions are shown, 1000, 1500, and 2000 rpm. Clearly the combustion of 2000 rpm is excellent with the flame failing to reach the extremity of the chamber only 5% of the time. At the lower speeds the burning is progressively less complete. At these low speed conditions day to day variation in combustion was quite large as illustrated by the approximate range of the data. Numerous data points were observed outside of the bands at 1000 and 1500 rpm and indicated that combustion is certainly inconsistent at these test conditions at probes 2 and 3.

Also, as expected, the frequency of misfire increased with distance from the spark source. The lack of burning at probe 3 is of particular significance because the density of the unburned mixture in this region is high. The last portion of the charge contains a disproportionately greater share of the fuel.

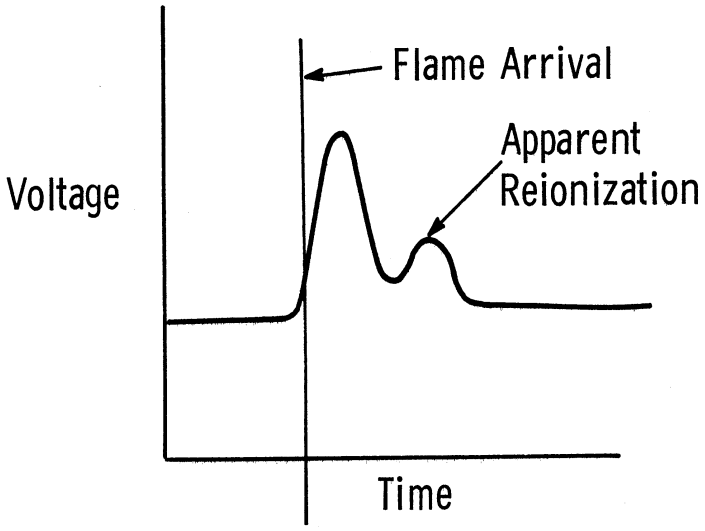

Figure 37. Schematic of multiple ionization during the traverse of a single flame front past an ionization probe.

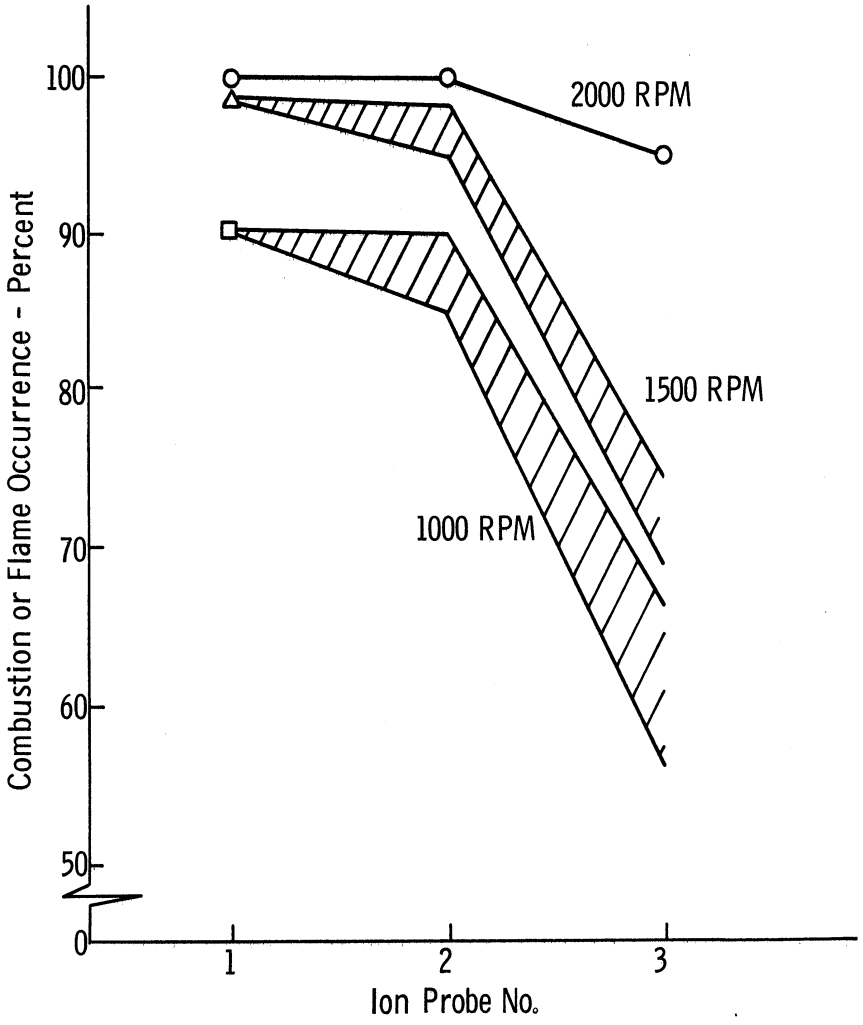

Figure 38. Results of misfiring test in cylinder 2.

Generally the ion probe technique was judged effective as a means for measuring misfiring or incomplete burning. It is not a simple system to use in this application because of the signal conditioning required and certain difficulties associated with the engines C-D ignition system.

IV. CONCLUSIONS AND OBSERVATIONS

A. MISFIRING MEASUREMENT—IONIZATION TECHNIQUE

1. Misfiring is a major source of the unburned hydrocarbon emissions at low speeds and light loads.

2. Above 2000 rpm, boat load burning was nearly complete. Only 5% misfire occurred at the most remote region of the combustion chamber, whereas at 1000 rpm the flame failed to reach this section of the chamber 40% of the time.

3. Care must be exercised with the ionization probe system to eliminate noise interference from the engine C-D ignition system.

B. SCAVENGING SIMULATION

1. Based on preliminary results there is little evidence that overscavenged fuel reacts with oxygen.

2. The exhaust gas hydrocarbon composition in the scavenging simulation closely resembles the composition of the fuel.

3. The photochemical reactivity of 2-stroke exhaust hydrocarbons per unit of hydrocarbon emission is approximately half as great as that for a 4-stroke engine.

C. CYLINDER SAMPLING

1. The Cox sampling valve appears to be an effective technique for the evaluation of several engine performance factors including misfiring, residual dilution of the charge, and cylinder fuel/air ratio.

2. Burning was observed to be slow, erratic, and on the average quite incomplete at the 1000 rpm, boat load test condition. Burning was less than 70% complete at 1000 rpm.

3. The sampled gas from the region near the combustion chamber wall appears to be representative of the bulk gases.

4. The FID/NDIR measured hydrocarbon ratio ranged from 1.4 to 3.3 and generally exceeded the range (1.3-1.7) observed in the exhaust system.

5. Residual dilution of the charge was significant and was between 30-35% at 1000 rpm, boat load, and approximately 20% at 3000 rpm, boat load.

V. APPENDICES

A. Circuit Parameters—Sample Valve Control Circuit

No.	RΩ	CμF	D	SCR	T
1	3.0K	.0033	IN750	C45E	2N1306
2	5.1K	.0033	IN914A	C45E	2N1306
3	5.1K	.0033	IN914A		
4	51	.05	IN914A		
5	1 K	10	IN914A		
6	3 K	20			
7	3 K	.01			
8	3 K	10			
9	5 K	10			
10	500	.01			
11	30 K	10			
12	30 K	.01			
13	5 K	320			
14	510	320			
15	30 K	150			
16	30 K	150			
17	5 K	150			
18	300	150			
19	30 K	35			
20	30 K	30			
21	500	30			
22	500				
23	500				
24	2 K (ea.)				
25	5				
26	50				
27	50				

B. Photochemical Reactivity Comparison of Exhaust Gas—
Four Cycle Engine vs. Simulation

First it is necessary to assume values for the relative reactivity of the major HC families in the exhaust. This is done on the basis of the ratio of the NO photochemical oxidation rate of HC family x to the photochemical rate of 2, 3, dimethyl-2-butene (Ref. 9).

$$RR_{HC_x} = \frac{\text{NO photo oxidation rate of } HC_x}{\text{NO photo oxidation rate of 2, 3, dimethyl-2-butene}}$$

The relative reactivity of the various families are approximated below.

Family	Relative Reactivity (RR)
paraffins	.5
aromatics	1.1
olefins	15

The total reactivity is defined by the following relationship.

$$\text{Total Reactivity} = \sum_x (RR_x)\ (\text{fraction } HC_x)\ (\text{total HC concentration})$$

As an example of the calculations, consider the preliminary simulation HC data from Table IV. For Case I, 4-cycle exhaust only, the total reactivity at probe 3 is:

Paraffins	(.5) x (.26) x (900 ppm) =	117
Aromatics	(1.1) x (.27) x (900 ppm) =	267
Olefins	(15) x (.47) x (900 ppm) =	4450
	Total	4834

Similarly, the total HC reactivity for the simulation of the "through scavenged" mixture, $\Gamma = .75$, at probe 3 is:

Paraffins	(.5) (.64) (9000)	=	2,880
Aromatics	(1.1) (.23) (9000)	=	2,260
Olefins	(15) (.13) (9000)	=	17,400
	Total		22,540

C. Fuel Composition—Exhaust Gas Calculation

If it is assumed that the over scavenged fuel (simulation) does not react chemically, it is possible to determine its HC family composition from the subtractive column data.

It is necessary to determine the family composition of both the 4-cycle exhaust only, Case I, and the total mixture, Case III.

The HC fraction from the 4-cycle combustion, x, is the ratio of the HC concentration from Case I to the HC concentration of Case III. The HC fraction of the unburned fuel is then 1-x.

For example, from probe 3 data, the following proportions are determined.

$$x = \frac{900}{9000} = .1$$

$$1-x = .9$$

Let a, b, and c be the paraffinic, aromatic, and olefinic fraction of the fuel, respectively. The fractions can be evaluated according to the following relationships.

$$(\text{Fraction } HC_i \text{ in fuel})(1-x) + (\text{fraction } HC_i, \text{ Case I})(x)$$
$$= (\text{Fraction } HC_i, \text{ Case III})$$

As an example, the fuel composition is calculated from the simulation data, Table IV.

Paraffinic fraction	.9a + .27(.1)	=	.62	a	= .67
Aromatic fraction	.9b + .28(.1)	=	.27	b	= .27
Olefinic fraction	.9c + .45(.1)	=	.1	c	= .06

These results fall within the allowable composition range of Indolene test fuel.

D. Calculation of Residual Dilution of Charge and Completeness of Combustion

First let us divide the gas samples into two groups—pre-combustion and post-combustion. The pre-combustion gases consist of two basic components: fuel/air mixture (fraction y) and post-combustion products or residual (fraction 1-y). Similarly, the post-combustion products can be separated into two components: pre-combustion gases or charge* (fraction x) and the complete products of combustion (fraction 1-x). This distribution is illustrated schematically below.

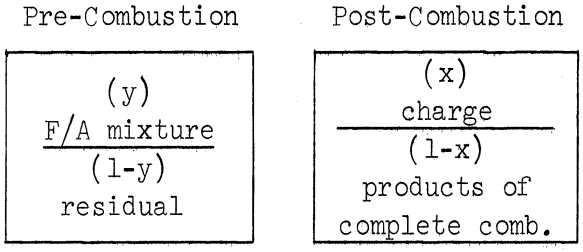

The concentration of CO_2, CO, and O_2 in the pre- and post-combustion gases are assigned the following symbols.

	Pre-Combustion	Post-Combustion
CO_2	(D)	(A')
CO	(E)	(B)
O_2	(F')	(C)

In the unburned mixture CO_2 and CO are not present and O_2 exists in the volume fraction .21 x 1/(1 + F/A), where the F/A ratio is obtained from the CO_2/CO ratio and the appropriate combustion chart.

*The charge is defined as the mixture of fuel, air, and residual.

The residual fraction or exhaust dilution (1-y) can be determined from either of the following relations:

$$CO_2 \quad A'(1-y) = D$$

$$CO \quad B(1-y) = E$$

$$O_2 \quad .21\left(\frac{1}{1 + F/A}\right)(y) + (C)(1-y) = F'$$

As an example of the calculations, let us consider the average pre- and post-combustion data from 2000 rpm, boat load (cylinder 2, 100 HP engine) which is summarized below:

	Pre-Combustion	Post-Combustion	
CO_2	D = 2.5%	A' = 9.1%	F/A = .091
CO	E = 2.2%	B = 7.3%	
O_2	F' = 15.4%	C = .5%	
CO_2	1-y = 2.5/9.1	= .275	
CO	1-y = 2.2/7.3	= .30	
O_2	.21 (1/1 + .091)y + .5 (1-y) = 15		1-y = .275

Thus three different calculations are presented for the determination of the residual dilution of the fresh fuel/air mixture using three separate exhaust gas analyses. Their close agreement strengthens the validity of the technique and provides a valuable cross check.

The fraction of charge burned or the completeness of burning is the

fraction (x) of the post-combustion gases. Conversely, the fraction unburned is (1-x). One key additional set of data is needed for this calculation; the CO_2, CO, and O_2 concentration in the complete products of combustion. These can be determined from the appropriate combustion chart if the combustion fuel/air ratio is known. With the rich mixture used in the 2-cycle engine, the concentration of O_2 is very close to zero ($O_2 \approx 0\%$). The CO_2/CO ratio can be utilized to define the F/A ratio and then the complete product's fraction of CO_2 and CO can be found. There is, however, one major potential error associated with this analysis. Even a slight error in the estimate of F/A ratio can result in a major error in the CO_2 and CO fraction obtained from the combustion products chart. For this reason, the results based on CO_2 and CO data were rejected.

The following relationship with the O_2 data is applicable:

$$F'(1-x) + 0\%\,(x) = C$$

As an example of this calculation consider the results at 1000 rpm.

Pre-combustion O_2 F = 15.6%

Post-combustion O_2 C = 5.4%

Fraction unburned = $1-x = \frac{5.4}{15.6} = .345$

or the fraction burned = $x = .655$

The pre- and post-combustion HC data can also be used but is believed to

be less reliable because of the potential inaccuracy of the analyzer at the high HC concentrations of the pre-combustion gases. Also, it is questionable whether the assumption that the complete products consist of 0% HC is valid with very rich mixtures and a small error in the post-combustion HC measurement taken from the quench zone may significantly alter the final calculations. The calculation procedure is indicated below

$$(1-x)\ HC_{pre} = HC_{post}$$

E. Sample Data Set—Misfiring Analysis

RPM	BHP	Engine Revs.	Combustion Count			Percent Misfiring		
			I.G.* #1	I.G. #2	I.G. #3	I.G. #1	I.G. #2	I.G. #3
2000	boat load	1006	1008					
2000	boat load	1005	1007					
2000	boat load	998		1007				
2000	boat load	995		999				
2000	boat load	1004		1009				
2000	boat load	3004		3017				
2000	boat load	1071			1007			5.5
2000	boat load	1057			1003			5.0
2000	boat load	1060			1002			5.2
1500	boat load	1009	1004			.5		
1500	boat load	1011	1004			.7		
1500	boat load	1026		1005			2.1	
1500	boat load	1033		1004			2.8	
1500	boat load	1365			1004			28.5
1500	boat load	1375			1003			29.0

*I.G. = ion gap.

VI. BIBLIOGRAPHY

1. Babcock, L. R., "A Combined Pollution Index for Measurement of Total Air Pollution," APCA Journal, Vol. 20, No. 10, Oct. 1970, pp. 653-659.

2. "Control of Air Pollution from New Motor Vehicles and New Motor Vehicle Engines," Federal Register, Vol. 35, No. 21, Nov. 1970.

3. Cole, D. E., "Two Stroke Gasoline Engine Exhaust Emissions," ORA Report 34856-2-F, The University of Michigan, 1970.

4. Sorenson, S. C., Myers, P. S., and Nyehara, O. A., "The Reaction of Ethane in Spark Ignition Engine Exhaust Gas," SAE paper 700471, presented at the SAE Mid-Year Meeting, June 1970.

5. Sigsby, J. E. and Klosterman, D. L., "Application of Subtractive Techniques to the Analysis of Automotive Exhaust," Environmental Science and Technology, Vol. 1, No. 4, April 1967, pp. 309-314.

6. Eltinge, L., Marsee, F. J., and Warren, A. J., "Potentialities of Further Emissions Reduction by Engine Modification," SAE paper 680123, presented at the SAE National Meeting, January 1968.

7. Patterson, D. J., "Kinetics of Oxidation and Quenching of Combustibles in Exhaust systems of Gasoline Engines," Annual Progress Report No. 1, ORA 31083-1-P, The University of Michigan, Feb. 1970.

8. Caplan, J. D., "Smog Chemistry Points the Way to Rational Vehicle Emission Control," Transactions of the Society of Automotive Engineers, Vol. 74, 1966.

9. Jackson, M. W., "Effects of Some Engine Variables and Control Systems on Composition and Reactivity of Exhaust Hydrocarbons," Transactions of the Society of Automotive Engineers, Vol. 75, 1967.